JUNE 2014

IN COMPLIANCE™

THE COMPLIANCE INFORMATION RESOURCE FOR ELECTRICAL ENGINEERS

Things You May Not Have Heard About Shielding

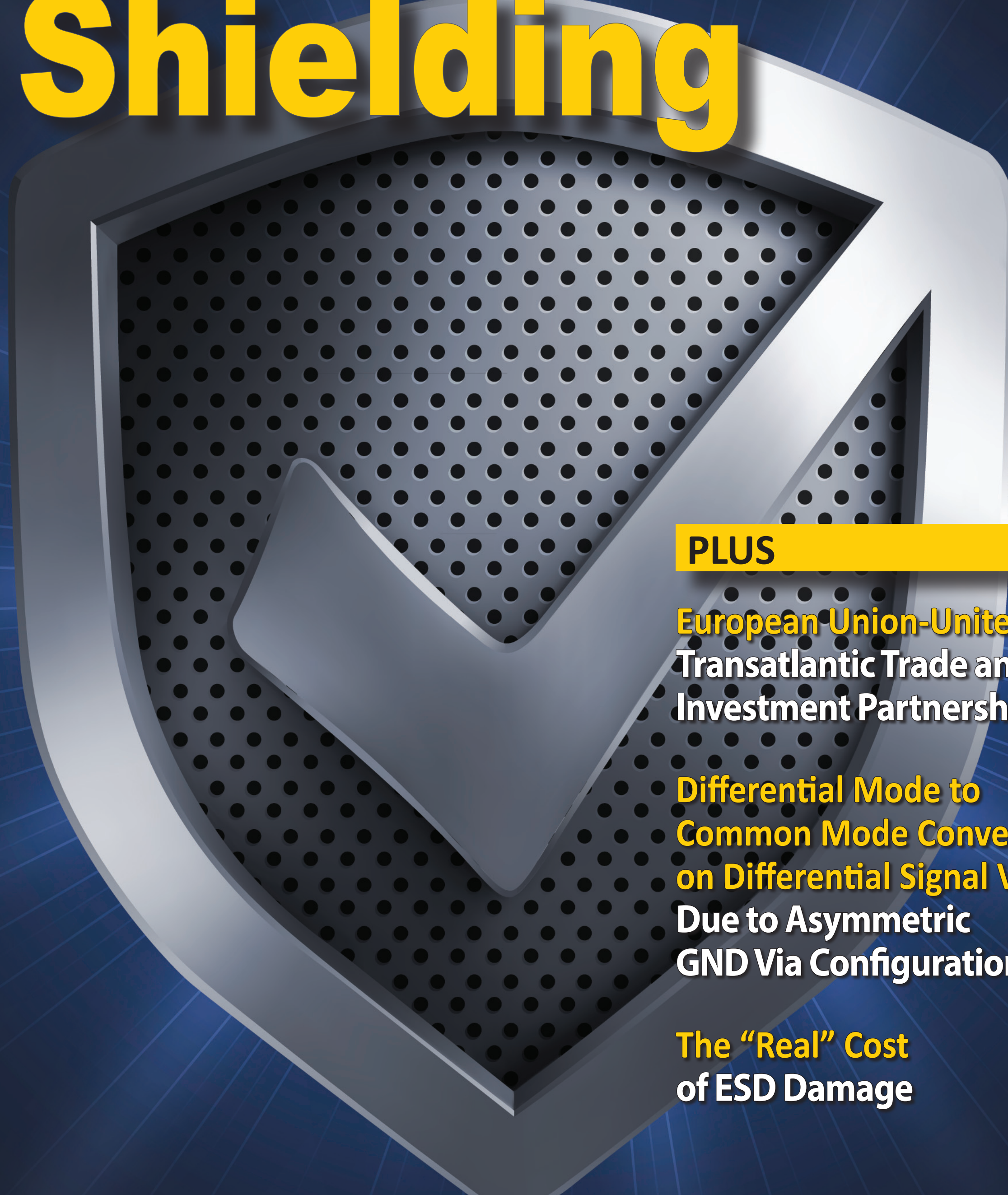

PLUS

European Union-United States Transatlantic Trade and Investment Partnership

Differential Mode to Common Mode Conversion on Differential Signal Vias Due to Asymmetric GND Via Configurations

The "Real" Cost of ESD Damage

GOT GAIN?

improve your overall system sensitivity

Preamplifiers

20 MHz - 40 GHz
8 Models

Low-Loss Cables

DC - 40 GHz
4 Models

Like milk and cookies, preamplifiers go together with high-frequency low-loss cables. As frequency requirements increase, so do the losses encountered in antennas, cables and test instrumentation. Our preamplifiers provide the necessary gain to overcome these losses. The signal level at the receiver must be high enough to produce useful data. A.H. Systems has both preamplifiers and low-loss cables to match all antennas to 2, 4, 7, 18, 26.5 and 40 GHz. Our custom length low-loss cables match these frequencies and can be assembled and delivered in 2 days. Why wait when you can have it all now.

Preamplifiers... And Cables too.

Innovation Quality Performance

Phone: (818)998-0223 ♦ Fax (818)998-6892
http://www.AHSystems.com
A.H. Systems

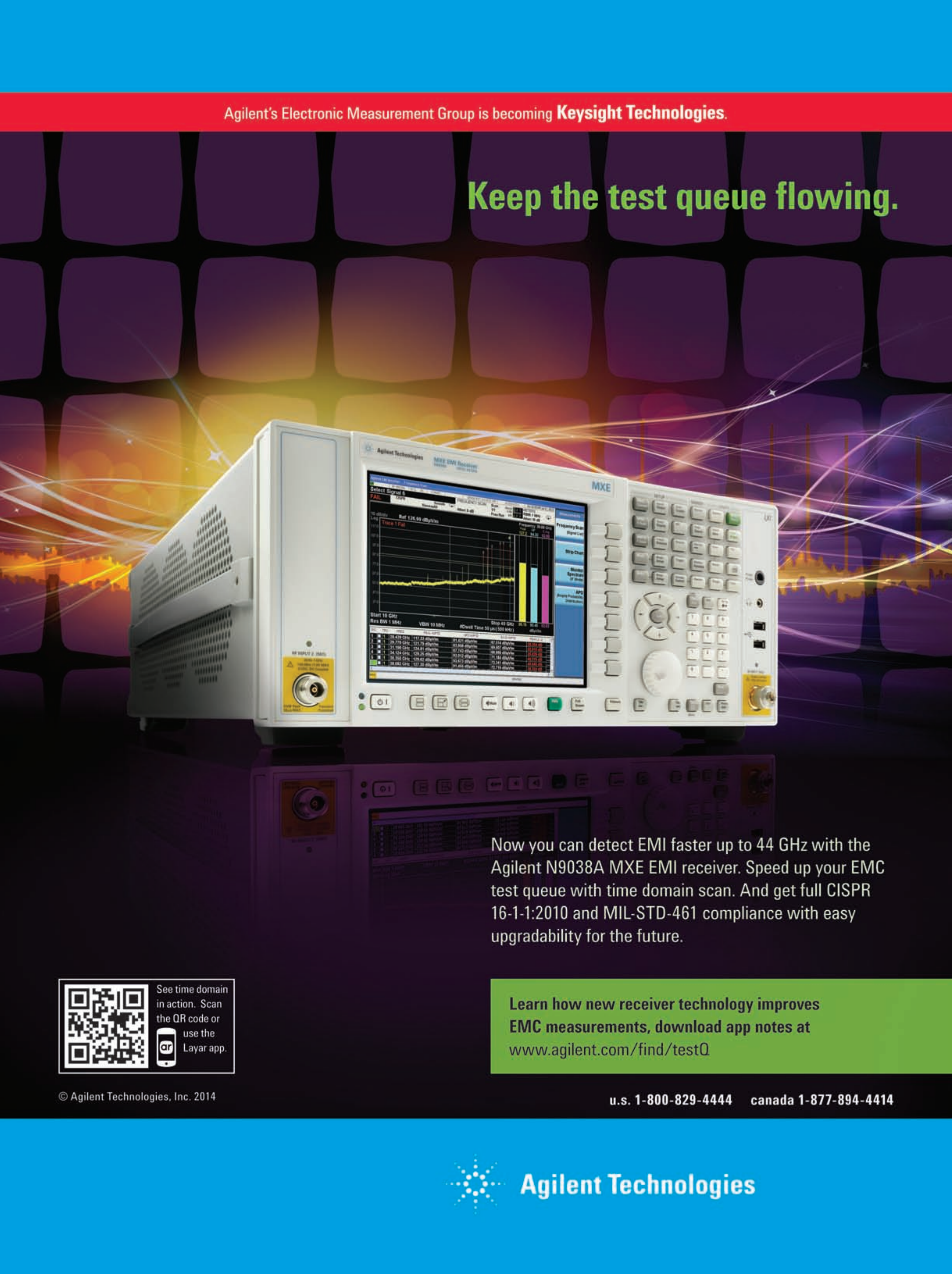
Agilent's Electronic Measurement Group is becoming Keysight Technologies.
Keep the test queue flowing.
Agilent Technologies
MXE EMI Receiver
MXE
Now you can detect EMI faster up to 44 GHz with the Agilent N9038A MXE EMI receiver. Speed up your EMC test queue with time domain scan. And get full CISPR 16-1-1:2010 and MIL-STD-461 compliance with easy upgradability for the future.
See time domain in action. Scan the QR code or use the Layar app.
Learn how new receiver technology improves EMC measurements, download app notes at www.agilent.com/find/testQ
© Agilent Technologies, Inc. 2014
u.s. 1-800-829-4444 canada 1-877-894-4414
Agilent Technologies

IN COMPLIANCE

In Compliance Magazine
ISSN 1948-8254 (print)
ISSN 1948-8262 (online)
is published by

Same Page Publishing Inc.
531 King Street, Suite 5
Littleton, MA 01460-1279
tel: (978) 486-4684
fax: (978) 486-4691

editorial staff

editor/publisher Lorie Nichols
lorie.nichols@incompliancemag.com
(978) 873-7777

production director Erin Feeney
erin.feeney@incompliancemag.com
(978) 873-7756

reality engineering contributing editor Mike Violette
mikev@wll.com
(978) 486-4684

publishing staff

director of business development Sharon Smith
sharon.smith@incompliancemag.com
(978) 873-7722

national sales manager Shellie Johnson
shellie.johnson@incompliancemag.com
(404) 991-8695

marketing communications strategist Ashleigh O'Connor
ashleigh.oconnor@incompliancemag.com
(978) 873-7788

marketing communications specialist Heather Stehman
heather.stehman@incompliancemag.com
(978) 873-7710

circulation manager Alexis Harrington
alexis.harrington@incompliancemag.com
(978) 873-7745

subscriptions

In Compliance Magazine subscriptions are free to qualified subscribers in North America.

Subscriptions outside North America are $129 for 12 issues. The digital edition is free.

Please contact our circulation department at circulation@incompliancemag.com

advertising

For information about advertising contact:
Sharon Smith at 978-873-7722
sharon.smith@incompliancemag.com

CONTENTS

June 2014

Volume 4 • Number 6

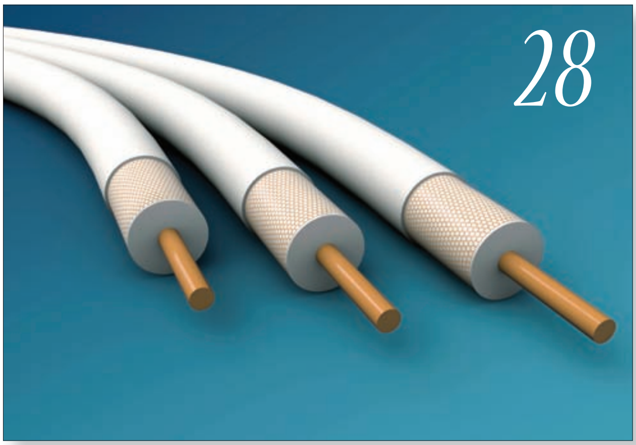

News in Compliance

FCC News

Peavey Pays $225,000 for Marketing Unauthorized Devices

Peavey Electronics Corporation of Meridian, MS has entered into a consent decree with the Federal Communications Commission (FCC), following an investigation into the company's compliance with FCC rules pertaining to the marketing of electronic devices.

According to a Consent Decree issued in April 2014, a 2011 investigation by the Commission's Spectrum Enforcement Division determined that certain digital electronic devices manufactured and/or marketed by Peavey did not include labeling consistent with FCC requirements, and that user manuals accompanying some devices did not include required consumer disclosure statements.

As part of a negotiated settlement with the Commission, Peavey has agreed to make a voluntary contribution of $225,000 to the U.S. Treasury. In addition, the company agreed to develop and implement a plan to ensure future compliance with the FCC's equipment marketing requirements and to establish a compliance training program for employees. Finally, Peavey will be required to file regular compliance reports with the Commission over the next three years.

The complete text of the Commission's Enforcement Order against Peavey Electronics is available at incompliancemag.com/news/1406_01.

FCC Seizes Pirate Radio Station Equipment

The Enforcement Bureau of the Federal Communications Commission (FCC) has recently stepped up its activities against operators of illegal radio stations, as evidenced by two separate instances involving the seizure of radio transmission equipment.

In New York, FCC agents and Deputy U.S. Marshalls seized equipment in Manhattan and the Bronx allegedly used by two separate pirate radio station operators to illegally broadcast programming on 94.5 and 94.9 MHz. The raids were conducted under warrants issued by the Office of the U.S. Attorney for the Southern District of New York, pursuant to FCC complaints and forfeiture orders.

Separately, in Boston, radio transmission equipment used by three pirate radio stations were seized under warrants issued by the United States Attorney's Office for the District of Massachusetts. The pirate radio stations were operating on FM frequencies in Boston, Mattapan and Dorchester, as well as Everett and Brockton, despite multiple warnings issued by the FCC to the station operators to cease broadcasting operations.

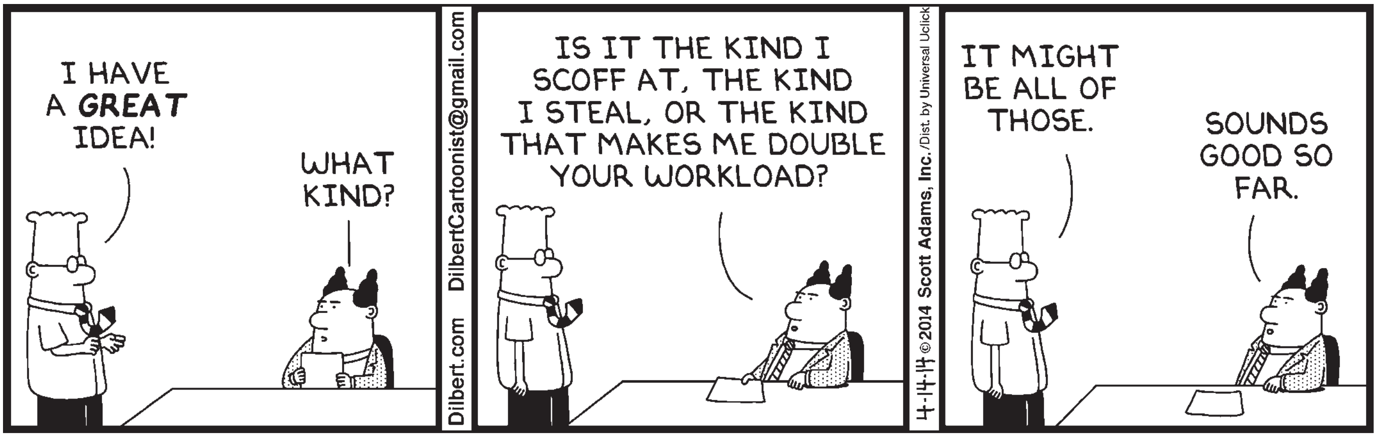

News in Compliance

FCC News

The United States Attorney's Office for the District of Massachusetts has reportedly executed eight separate forfeiture actions since 2011 against illegal radio stations operating in the Boston area.

The Communications Act of 1934 makes it unlawful to operate radio broadcasting equipment outside of prescribed limits without a license from the FCC, and authorizes the Commission to seize and forfeit any equipment used for such purposes.

FCC Proposes New "Innovation Spectrum" for Broadband Radio Service

The Federal Communications Commission (FCC) has released proposed rules for a new Citizens Broadband Radio Service that it says would promote a diverse array of network technologies and allow the exploration of new methods of spectrum sharing.

According to a Further Notice of Proposed Rulemaking issued in April 2014, the new radio service would utilize spectrum between 3550 and 3700 MHz, and consist of a three-tiered spectrum access and sharing model that would include federal and non-federal incumbent license holders, priority access licensees, and general authorized users.

The Commission says that its proposal would protect incumbent licensees from harmful interference while also making available target priority access licenses for various uses, such as broadband mobile services. General authorized access would be permitted within a reserve amount of spectrum for other consumer and business use, including advanced home wireless networking services. Activity within the proposed Service spectrum would be managed by a "spectrum access system," a dynamic database that would manage access and operations across the three tiers.

If successful, the Commission says that the spectrum sharing model utilized by the new Citizens Broadband Radio Service could be expanded to other spectrum bands, thereby increasing the overall availability of spectrum.

The complete text of the Commission's Notice is available at incompliancemag.com/news/1406_02.

You Can't Make This Stuff Up

Police Social Media Plans Backfires

The New York Police Department is putting on a brave face after its efforts to use social medial to build a positive public image backfired.

According to Reuters News Service, the NYPD launched a hopeful social media campaign in April, inviting Twitter users to submit to #mynypd pictures of themselves with New York's finest and offering to post some of the submitted pictures to the Department's Facebook page.

However, within less than 24 hours, the hashtag had been tweeted more than 94,000 times, with most tweets showing images of alleged police brutality and violence against citizens. By the next day, the negative viral campaign had grown to include other police departments around the country, including Miami, Detroit, Los Angeles, and Chicago.

William Bratton, the New York Police Commissioner who was appointed to the office earlier this year, acknowledged that "the reality of policing is that oftentimes our actions are lawful, but they look awful." Nonetheless, Bratton said that he would continue the Twitter campaign, encouraging New Yorkers to "send us your photos, good or bad."

News in Compliance

European Union News

New List of Standards Issued for EU's Machinery Directive

The Commission of the European Union (EU) has issued an updated list of standards that can be used to demonstrate compliance with the essential requirements of its Directive 2006/42/EC, also known as the Machinery Directive.

The EU's Machinery Directive defines the essential health and safety requirements for a wide range of products, including: machinery and partly completed machinery; lifting accessories; chains, ropes and webbing; interchangeable equipment; removable mechanical transmission devices; and safety components.

The Directive's scope specifically excludes electrical and electronic products covered under Directive 2006/95/EC (the EU's so-called Electrical Safety Directive), including household appliances, audio and video equipment, informational technology equipment, and ordinary office machinery.

The extensive list of CEN and Cenelec standards for the Machinery Directive was published in April 2014 in the *Official Journal of the European Union* and replaces all previously published standards lists for the Directive.

The revised list of standards can be viewed at incompliancemag.com/news/1406_03.

EU Details Measurement Methods for Computer Eco-Design Requirements

The Commission of the European Union (EU) has issued a Communication detailing transitional measurement methods to be used to demonstrate compliance with its eco-design requirements for computers and computer servers.

Specific energy efficiency requirements for computers and computer servers are extensively detailed in Commission Regulation No 617/2013, an implementing regulation published in June 2013 under the provisions of the EU's Eco-Design Directive (2009/125/EC). However, qualified methods of measurements and calculations to assess compliance with these requirements were not detailed in the Regulation, necessitating the identification of transitional measurement methods.

The Communication regarding transitional measurement methods was published in April 2014 in the *Official Journal of the European Union*. It is expected that these transitional measurement methods will eventually be replaced by harmonized standards. Notice of harmonized standards that can be used to demonstrate compliance will be published in the *Official Journal* once they have been approved.

The complete text of the Commission's Communication regarding transitional measurement methods for the eco-design of computers and computer servers is available at incompliancemag.com/news/1406_04.

EU Commission Updates Standards List for PPE Directive

The Commission of the European Union (EU) has an updated list of standards that can be used to demonstrate conformity with the essential requirements of its Directive 89/686/EEC concerning personal protective equipment.

For the purposes of the Directive, personal protective equipment (or PPE) is defined as "any device or appliance designed to be worn or held by an individual for protection against one or more health and safety hazards." Specifically excluded from the scope of the Directive is equipment designed specifically for private use (such as seasonal outdoor clothing), equipment for use by armed forces or law enforcement personnel, and equipment intended for the protection or rescue of individuals on vessels or aircraft.

The extensive list of CEN and Cenelec standards was published in April 2014 in the *Official Journal of the European Union* and replaces all previously published standards lists for the Directive.

The complete updated standards list for the EU's PPE Directive is available at incompliancemag.com/news/1406_05.

CPSC News

Dyson Recalls Portable Electric Heaters

Dyson Inc. of Chicago, IL has announced the recall of nearly 340,000 Dyson-brand portable electric heaters manufactured in Malaysia.

Dyson reports that the portable electric heaters can develop an electrical short and overheat, posing a fire and burn hazard to consumers. The company has received reports of at least 82 incidents of the recalled heaters short-circuiting and overheating, along with four reports of heaters manifesting burned or melted internal parts. However, there have been no reports of injuries or property damage.

The recalled portable electric heaters were sold through major U.S. retailers, including Bed Bath & Beyond, Best Buy, Costco, Fry's, Kohl's, Macy's, Sears, and Target, as well as online through Abt.com, Amazon.com, Dyson.com, Groupon.com, HSN.com, QVC.com, and Walmart.com. The heaters were sold from September 2011 through March 2014 for about $400.

Dyson's recall also includes approximately 43,000 portable heater units sold in Canada.

Additional information about this recall is available at incompliancemag.com/news/1406_06.

Infant Video Monitors Recalled Due to Battery Issues

Summer Infant of Woonsockett, RI is recalling about 800,000 rechargeable batteries manufactured in China and used in the company's infant handheld color video monitors.

The company says that the rechargeable battery in the handheld video monitor can overheat and rupture, posting a burn hazard to consumers. Summer Infant reports that it has received 22 separate reports of overheated and ruptured batteries including some incidents involving smoke and minor property damage. However, there have been no reports of injuries.

The recalled rechargeable batteries were sold together with infant video monitors through mass merchants and independent juvenile specialty stores, as well as through online retailers, from February 2010 through 2012 for between $150 and $350. A 2011 recall of the same batteries addressed infant video monitors sold exclusively at Babies R Us retail stores.

Further details about this recall are available at incompliancemag.com/news/1406_07.

Playtex Recalls Power Adaptors Due to Electric Shock

Playtex Manufacturing, Inc. of Shelton, CT has recalled an unknown number of AC/DC power adaptors sold with its Playtex-brand Nurser Deluxe Double Electric Breast Pumps.

Playtex reports that the casing on some of the power adaptors may become loose and separate, potentially exposing consumers to the risk of an electrical shock. The company says that it has not received any reports of injuries related to the recalled power adaptors and has initiated the recall action "out of an abundance of caution."

The recalled adaptors were manufactured from November 2012 through July 2013, and were sold with Playtex Breast Pumps at nationwide specialty and online retailers. The adaptors were not sold separately.

More information about this recall is available at incompliancemag.com/news/1406_08.

Do you have news that you'd like to share with your colleagues in the compliance industry? We welcome your suggestions and contributions.

Send news items to the editor at editor@incompliancemag.com

REALITY Engineering

Millibels in the Wind

BY MIKE VIOLETTE

"Voiceless it cries,
Wingless flutters,
Toothless bites,
Mouthless mutters."
— J.R.R. Tolkien, *The Hobbit*

Radiometers are cool. Some are so cool they are cryogenically cool. They have to be really cool to do what they do. This is especially true for a bird called WindSat, a project that gave me a new appreciation for fragments of decibels and the remarkable engineering precision that is needed to see the wind.

WHERE SHE BLOWS?

How can you see the wind from space? And why would one? A few reasons to know what the wind is up to: storm-tracking, navigation needs, weather predication, and measuring climate change impact, to name a few.

The question is: How to do?

The answer is? Radiometry.

Innovations in electronics, radio frequency engineering, satellite technology and earth science converge within the area of Remote Sensing, which uses portions of the electromagnetic spectrum to image, measure and analyze at a distance. The techniques are used heavily in astronomy and, more and more, in observations of our planet.

Remote sensing is based on the physics that every object emits electromagnetic radiation (as long as they are warmer than minus 273.16°C). All matter above absolute zero is composed of vibrating molecules with various (complex) charge distributions. As these charges wiggle, according to Maxwell, electromagnetic radiation arises.

A *simple* radiometer can be had for $12.99. Putting the thing in the Sun spins the vanes in a partial vacuum. The energy from the Sun heats the black side of the vanes slightly, the heated air molecules

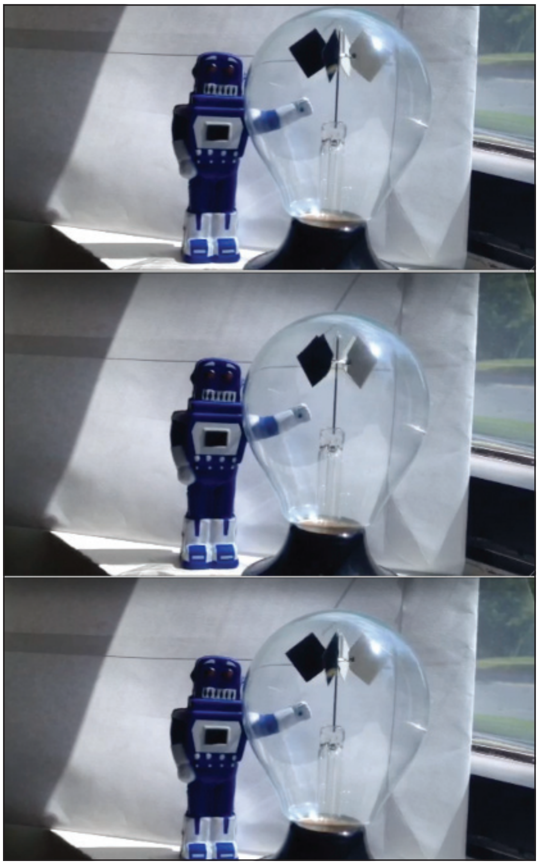

Figure 1

move away from the vane, and, to keep Newton happy, the vanes spin, suspended on a low-friction support. The spin rate depends on the amount of energy (sunlight) that hits the device (Figure 1).

For space-based observations, the energy that is reflected back from the Earth's surface can be gathered and measured, which allows a "picture" of the Earth to be developed. It just takes a few quanta of understanding.

MAX'S MEASUREMENTS

In the year 1900, Max Planck figured out the mathematical distribution for this energy and applied it to describe black-body radiation, which is the spectral energy that is emitted by, naturally enough, black bodies in thermal equilibrium.

Max postulated that the energy is directly proportional to frequency as $E = hf$, where h is Planck's constant (note: if you make up a formula, you get to name a constant after yourself), which is a teeny tiny number: 6.624×10^{-34} joule-seconds (f is the frequency in Hertz).

E then reduces simply to joules, a unit of energy. Max later developed an empirical model of black body radiation that is too complex to try to type up on my Mac, so I'll let you have a look yourself at the 420,000 Google returns you'll get if you search on "Planck's Law."

Figure 2

REALITY Engineering

Over a given area and frequency band, the energy unit is the **spectral radiance**, which is quantified as *watts per steradian per square meter*, which is a term that describes the energy flux over a certain amount of space. In the microwave region, it's tiny, but can be measured with the right radio receivers.

According to the science used to gather information about the wind at the surface of the planet (which can be used to measure other physical parameters such as soil moisture and ice coverage), performing *polarimetric radiometry* measurement yields something called the "Stokes Vector" or "Stokes Parameters" (see Figure 3). These parameters describe the polarization properties of the emitted radiation, which are essentially Cartesian representation of the wind vector plus a rotational component.[1]

The broadband energy that the Earth returns to space every second is a form of emissions that can be parsed into various frequency bands. The frequencies that best reveal wind data are in the 10 to 37 GHz range. Windsat, mentioned previously, has a horn feed bench that sips energy off a 1.8 m reflector. Thing is, to collect enough energy to make a good measurement, the bandwidths are whoppingly large, up to 2 GHz at the higher frequencies. Talk about a wide-open front end!

$$I_s = \begin{bmatrix} I \\ Q \\ U \\ V \end{bmatrix} = \begin{bmatrix} T_v \\ T_h \\ T_{45} - T_{-45} \\ T_{lc} - T_{rc} \end{bmatrix} = \begin{bmatrix} \langle E_v E_v^* \rangle \\ \langle E_h E_h^* \rangle \\ 2\,\mathrm{Re}\langle E_v E_h^* \rangle \\ 2\,\mathrm{Im}\langle E_v E_h^* \rangle \end{bmatrix}$$

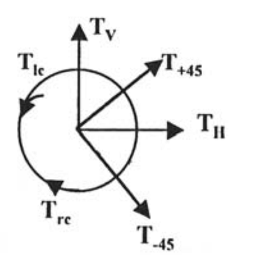

Figure 3

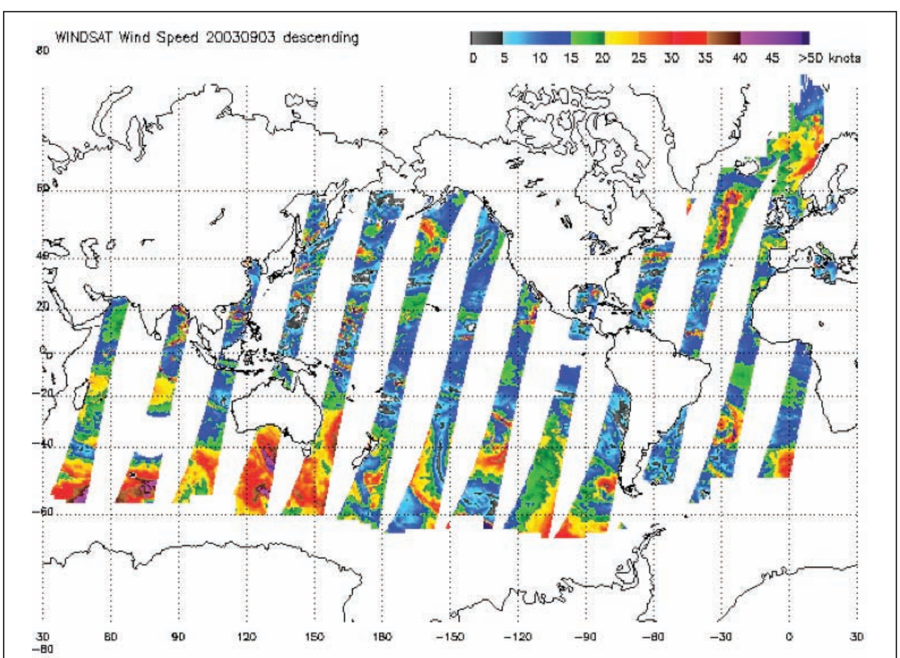

Figure 4

WINDSAT: SATELLITE-BASED OCEAN WIND SPEED AND DIRECTION SYSTEM

Our experience with flying radiometers was a dozen or so years ago. The Windsat project was developed by the Naval Research Center and launched in 2003 aboard a Titan II rocket as the primary payload of the Coriolis mission.[2]

The Windsat satellite runs around the planet in a more-or-less polar orbit at 830 km and is in a "Sun Synchronous Orbit" which means that her flight is tuned for maximum sunlight on the Earth, except for 'eclipse season' which occurs a little less than a quarter of a year. It takes the spacecraft just about 100 minutes to go 25,000 miles, which is a 16,000 miles per hour clip. Meanwhile, she's spinning around once every 2 seconds.

By scanning the surface of the earth as it rotates under her, Windsat can image 83% of the Earth's surface in one day. To get the remaining patches, a full four days are necessary (see Figure 4). A "swath" of 1400 km is imaged on each path, and the images are merged over multiple passes.[3]

Our work was on the EMC review of the spacecraft design during Preliminary Design Review (PDR). In addition to the *normal* EMC stuff (antenna coupling predictions, test specification writing) we were to take a look at system noise calculations.

Receiver performance is limited by the amount of self-generated noise in the receiver electronics. This is due to the kTB thermal noise caused by the electronics bumping around, which is proportional to the physical temperature of the device. So, it is customary to rate communications receiver sensitivity in terms of **noise temperature**, which is related to **noise figure.**

Noise figure and noise temperature are related where:

$$NF\ (dB) = 10Log[(T_{Noise}K/\ T_{Ref}K) + 1]$$

Where T_{Ref} is a reference temperature, typically 290K (around 17°C).

The lower the noise temperature/figure, the lower a signal the system can measure. At absolute zero, theoretically, the noise figure goes to zero.

HERE'S WHERE IT GETS A LITTLE CRAZY

As you might imagine, the wind whipping on the surface of the planet some 500 miles away doesn't throw off much radiation energy. To gather those RF whispers, the receivers are super sensitive. Control of noise figure is paramount. To give an idea of the miniscule amount of radiation that is made by the wind, a glance at the specifications for the receiver noise temperatures is interesting. For each of the bands, stretching from 6.8 GHz to 37 GHz, the specified noise temperature is less than 0.2K, zero K being as low as you can go.

How low is 0.2K? Well, consider that a noise temperature of 0.2K is equivalent to a noise figure of 0.027 dB or **2.7 millibels**.

When Norm was crunching the numbers on these calculations, on layers of legal pads, I was incredulous. Why carry the dB calculations out to three decimal points?

TBT, if you lose a part of a dB somewhere in a radiometer, your readings will be crushed.

With this fine precision, WindSat can measure the sea surface temperature with an accuracy of 0.5°C, wind speed with accuracy of ±2 m/s and wind direction with an accuracy of ±20°. Astonishing.

For EMC engineers, decibels are a little like sand, plentiful and cheap. If you lose or gain a handful here or there, it really doesn't matter that much. But for radiometer engineers, dBs are like jewels: you watch every carat, even down to the *millibel*.

ENDNOTE

Windsat was originally designed to fly for three years. After 11 years, according to Windsat's web page, "WindSat is operating normally." *Really cool.*

REFERENCES

1. WindSat Preliminary Design Review, Naval Research Laboratory, 10 June 1998.
2. www.nrl.navy.mil/WindSat/
3. "WindSat — Space Borne Remote Sensing of Ocean Surface Winds," Peter Gaiser, Mike Bettenhausen, Zorana Jelenak, Elizbeth Twarog, and Paul Chang, Naval Research Laboratory, Washington DC, NOAA/NESDIS, Camp Springs, MD, 8 February 2005.

(the author)

MIKE VIOLETTE
is President of Washington Labs and Director of American Certification Body. He can be reached at mikev@wll.com if you want to shoot the breeze.

TECHNICALLY Speaking

Resistor Value for Measuring Leakage Current

Product Safety Newsletter - September/October 1988

BY RICHARD NUTE

Dear Readers,
Over the past couple of years many of you have requested that we include more product safety related information in our issues. Of particular interest has been Rich Nute's series of "Technically Speaking" articles. And so… Mr. Nute has graciously agreed to work with us to bring you that series! Look for his column each month. We hope you enjoy the addition of "Technically Speaking" to the pages of In Compliance.

Furor and controversy are words which describe the process by which standards committees decide the value of the resistor in the leakage current measuring network.

However, the different specified resistor values create no more than a 6.25% error for the value of the leakage current.

More furor and controversy surround the selection of the resistor tolerance. The resistor tolerance creates almost the same percentage error in the measured value.

Still more furor and controversy occur when we compare the ANSI, UL, CSA and IEC measuring circuits.

The ANSI, UL, CSA and IEC circuits are demonstrably identical; all four give the same measured value.

RESISTOR VALUE

Different standards specify different values for the current-sampling resistor in the current-measuring circuit for electric shock current and leakage current. Examples of these different values are shown in Table 1.

Current-sampling resistor	Standard	Paragraph
500 ohms	UL 1270	19.1
1000 ohms	UL 544	27.13
1500 ohms	UL 478	28A.6
2000 ohms	UL 1459	48.6

Table 1

WHAT DIFFERENCE DO THESE VALUES MAKE?

Let us assume that we are measuring 0.5 milliampere of leakage current from a 120-volt product. To have leakage current we must have a circuit consisting of a voltage source, a series impedance, the current-sampling resistor (1500 ohms), and a return path (ground). See Figure 1.

We know E (120 volts) and I (0.5 mA). Using Ohm's law, the total resistance in the circuit, including the 1500-ohm current-sampling resistor is:

$$R = \frac{E}{I}$$

$$R = \frac{120}{0.0005}$$

$$R = 240{,}000 \text{ ohms}$$

Subtracting the 1500-ohm current-sampling resistor, we have a source resistance of 238.5 kilohms. Using this value, we can calculate the current when using other values of current-sampling resistor.

And, we can repeat the calculations for a 240-volt source.

And, we can repeat the calculations for 3.5 milliamperes and 5.0 milliamperes leakage current.

What do these data mean? Essentially, we have a current source. This means that the current is nearly independent of the load which, in this case, is the current-sampling resistor.

The worst-case error is +6.25%. This means that a manufacturer could test leakage current with an

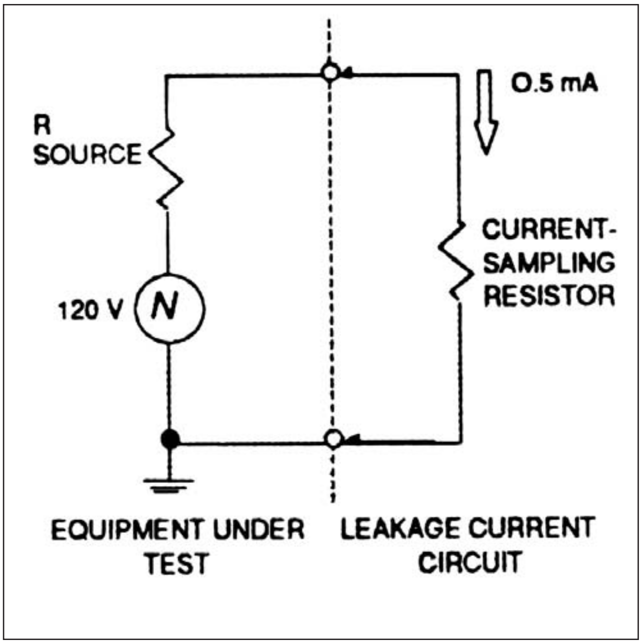

Figure 1: Leakage Current Circuit

ordinary ammeter, knowing that the ammeter reading is higher than the reading with a 1500-ohm resistor. If a manufacturer used the ammeter and the actual limit value, 0.5, 3.5 or 5.0 milliamperes, he would have a small guard-band such that his measurements would always be pessimistic.

So, where only power-line frequency appears in the leakage current, why go to the trouble of using the resistor? If it passes with the ammeter, it will pass with the resistor!

Why all the fuss about the value of the resistor?

RESISTOR TOLERANCE

Let us assume that we are again measuring 0.5 milliampere of leakage current from a 120-volt product. Recall from the discussion of resistor value, the source impedance is 238.5 kilohms when leakage current is 0.5 milliampere and the current-sampling resistor is exactly 1500 ohms.

In this case, assume the current- sampling resistor is a 1500-ohm, 5% resistor. Let us further assume that the resistor is at the low end of its tolerance, -5%. The resistor value therefore

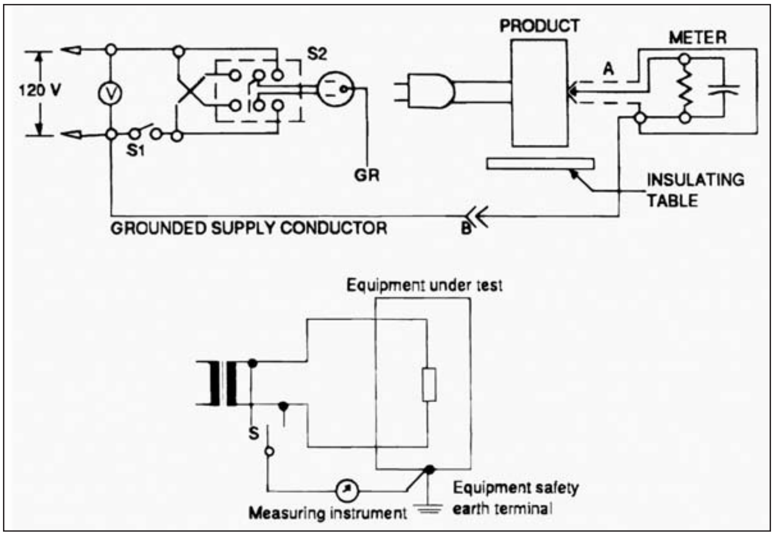

Figure 2a: Original Circuits, UL - IEC

is 1425 ohms. Using Ohm's law, the current in the circuit is:

$$I = \frac{E}{R}$$

$$I = \frac{120}{235{,}500 + 1425}$$

$$I = \frac{120}{239925}$$

I = 0.5002 milliampere

The actual voltage across the 1425-ohm resistor is:

$E = (I)\,(R)$
E = (0.5002) (1425)
E = 0.713 volts

If we now calculate the value of leakage current using the nominal value of the resistor rather than the actual value, we get:

$$I = \frac{E}{R}$$

$$I = \frac{0.713}{1500}$$

I = 0.475 milliampere

This is very nearly the same error as the resistor tolerance, 5%.

MEASURING CIRCUITS

The UL and IEC measuring circuits are shown in Figure 2a. In a progression of figures, the circuits are simplified to their essential elements-ultimately showing the equality of the UL and IEC circuits.

Figure 2b adds the source to the UL circuit as is already shown in the IEC circuit. Note that the UL circuit has its neutral grounded, while the IEC does not. The IEC circuit has the equipment grounded, while the UL does not.

Figure 2c deletes the ground from both the UL and the IEC circuits. Since there is only one connection to ground in both circuits, there can be no current in the ground, so the grounding is extraneous to the measurement.

Figure 2d simplifies the UL circuit by deleting the plug and socket.

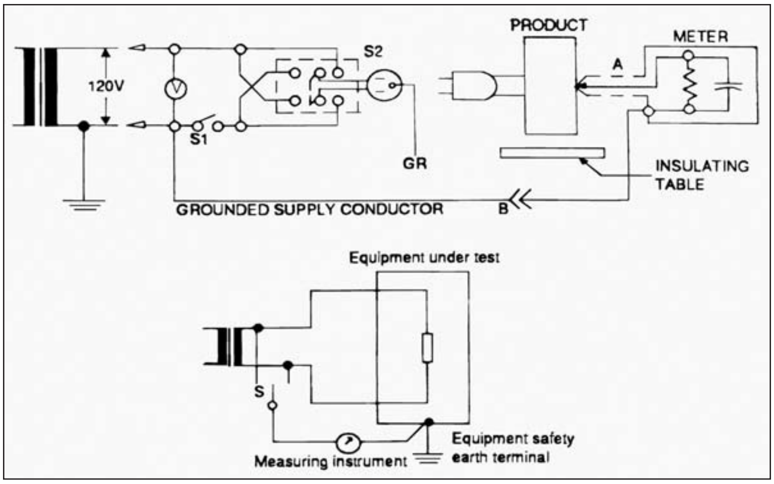

Figure 2b: Add Source to UL

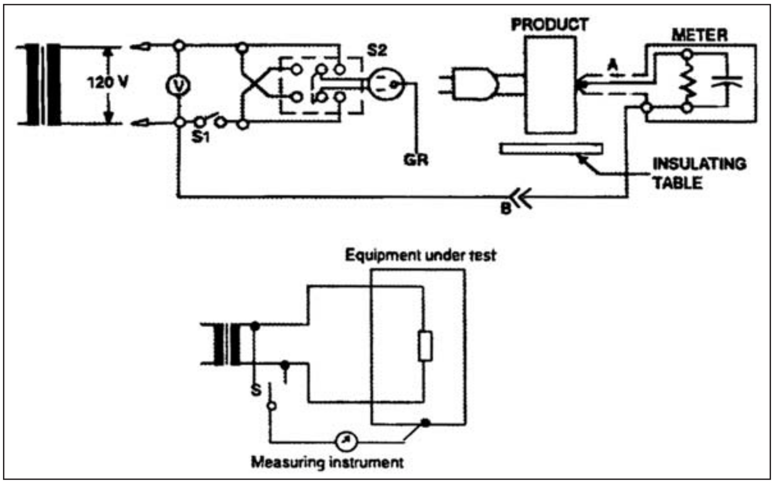

Figure 2c: Delete Grounding

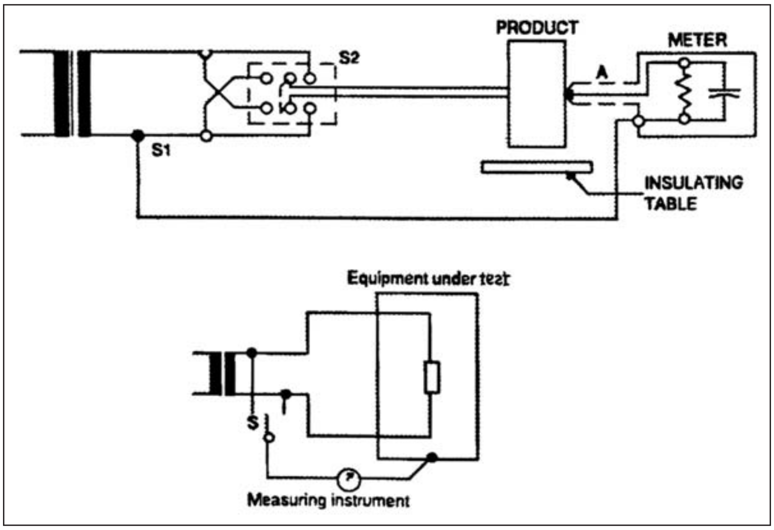

Figure 2d: Simply UL

TECHNICALLY Speaking

Figures 2e and 2f show the normal and reverse polarity positions, respectively, of the UL and IEC polarity switches.

CAPACITOR

Next, let's examine the effect of the 0.15 microfarad capacitor in parallel with the current-sampling resistor. Capacitive reactance is given by:

$$X_C = \frac{1}{2\pi f C}$$

$$X_C = \frac{1}{2\pi(60)(0.15)(10^{-6})}$$

X_C = 17.7 kilohms

The parallel network of 17.7 kilohms and 1.5 kilohms resolve to an impedance of 1.38 kilohms. This is less than 10% effect at 60 hertz.

The capacitor is useful only when the leakage current includes high-frequency currents, which the capacitor serves to shunt around the current-sampling resistor. If the capacitor is not used, then the measurement is higher than it would be with the capacitor.

CONCLUSION

The value of the current-sampling resistor in measuring leakage current at power-line frequencies is of negligible consequence to the measurement. The use of an ordinary ammeter will always give a pessimistic and worst-case value for leakage current. If your product has an acceptable leakage current with an ammeter, then it will have an acceptable leakage current with the standard current-sampling measurement circuit. And, there is no difference between the UL and IEC measuring circuits. Perhaps furor and controversy are not necessary after all! IN

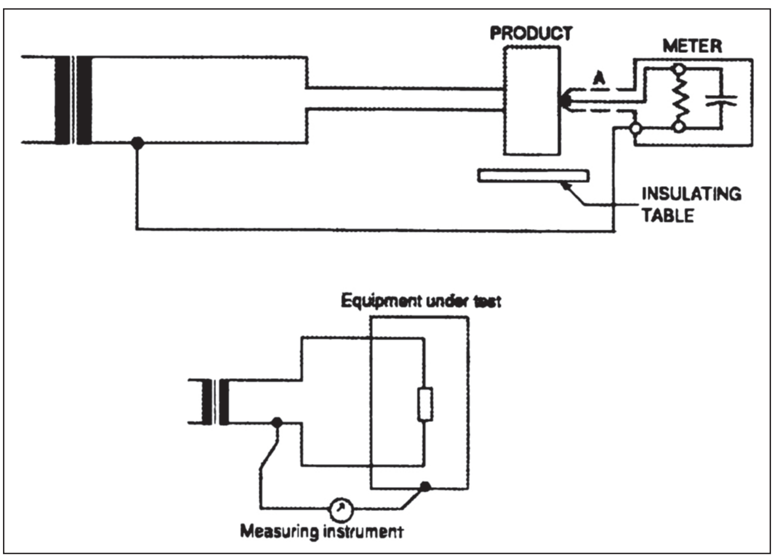

Figure 2e: Normal Polarity

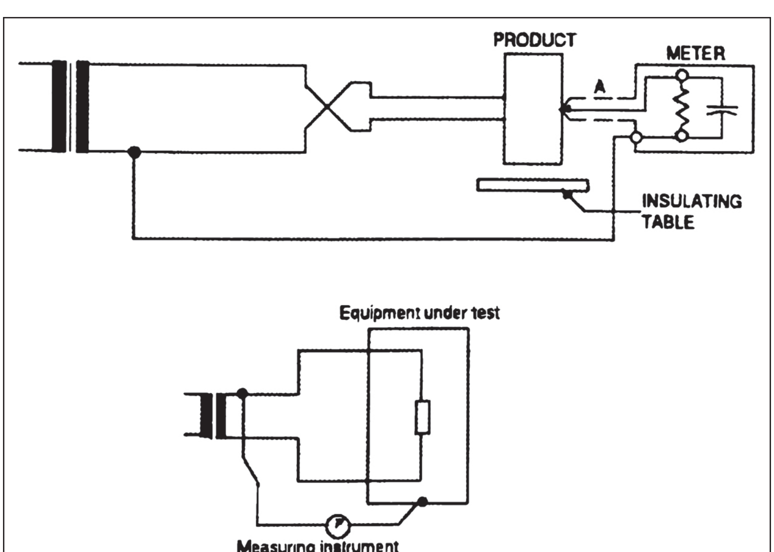

Figure 2f: Reverse Polarity

(the author)

RICHARD NUTE
is a product safety consultant engaged in safety design, safety manufacturing, safety certification, safety standards, and forensic investigations. Mr. Nute holds a B.S. in Physical Science from California State Polytechnic University in San Luis Obispo, California. He studied in the MBA curriculum at University of Oregon. He is a former Certified Fire and Explosions Investigator.

Mr. Nute is a Life Senior Member of the IEEE, a charter member of the Product Safety Engineering Society (PSES), and a Director of the IEEE PSES Board of Directors. He was technical program chairman of the first 5 PSES annual Symposia and has been a technical presenter at every Symposium. Mr. Nute's goal as an IEEE PSES Director is to change the product safety environment from being standards-driven to being engineering-driven; to enable the engineering community to design and manufacture a safe product without having to use a product safety standard; to establish safety engineering as a required course within the electrical engineering curricula.

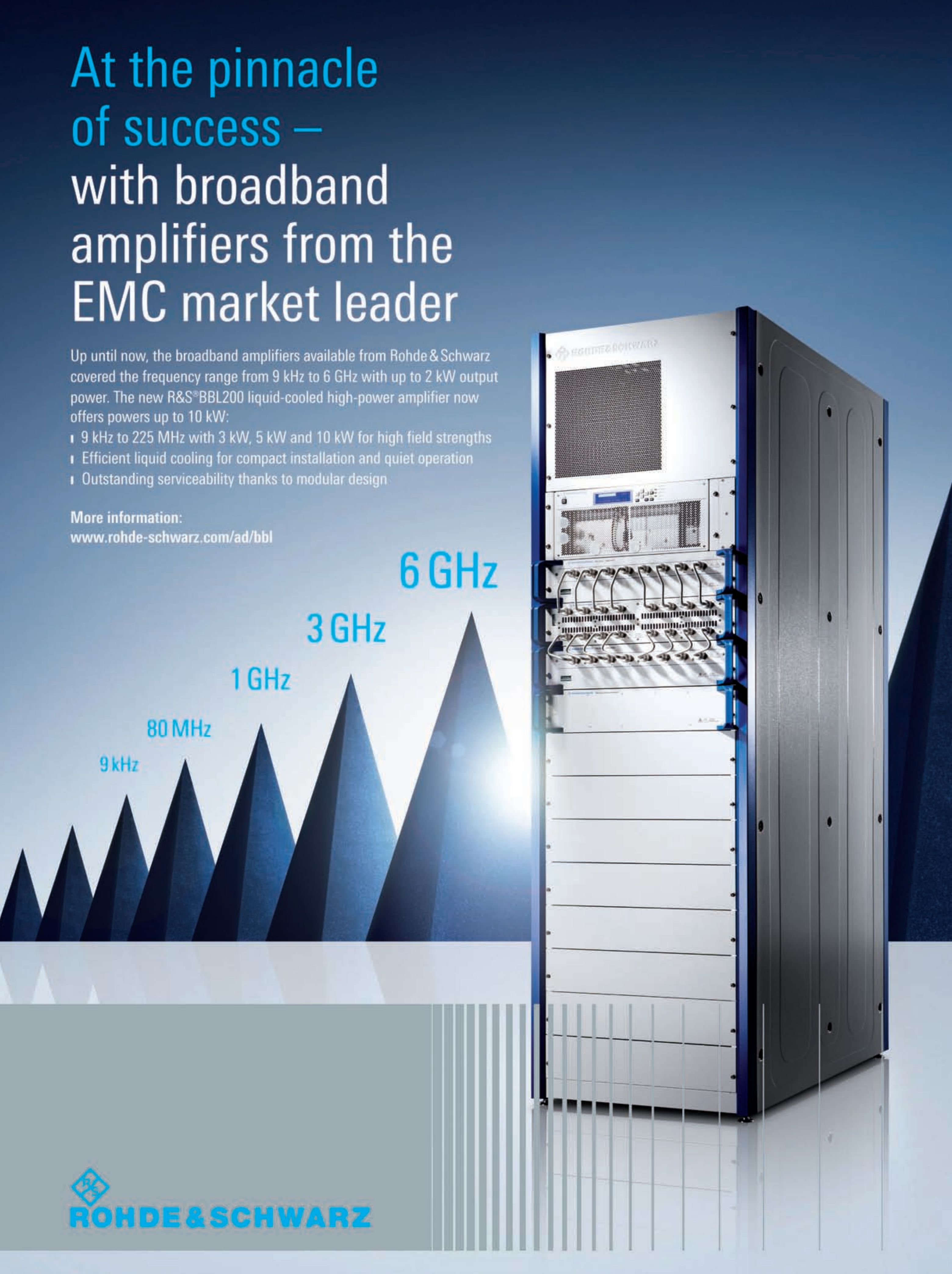
At the pinnacle of success – with broadband amplifiers from the EMC market leader
Up until now, the broadband amplifiers available from Rohde & Schwarz covered the frequency range from 9 kHz to 6 GHz with up to 2 kW output power. The new R&S®BBL200 liquid-cooled high-power amplifier now offers powers up to 10 kW:
9 kHz to 225 MHz with 3 kW, 5 kW and 10 kW for high field strengths
Efficient liquid cooling for compact installation and quiet operation
Outstanding serviceability thanks to modular design
More information:
www.rohde-schwarz.com/ad/bbl
6 GHz
3 GHz
1 GHz
80 MHz
9 kHz
ROHDE&SCHWARZ

MR. Static

Environmental ESD: Part 1

The Atmospheric Electric Circuit

BY NIELS JONASSEN, sponsored by the ESD Association

An understanding of the atmospheric electric circuit provides an insight into the processes underlying ESD events.

INTRODUCTION

Associate Professor Neils Jonassen authored a bi-monthly static column that appeared in *Compliance Engineering Magazine*. The series explored charging, ionization, explosions, and other ESD related topics. The ESD Association, working with *IN Compliance Magazine* is re-publishing this series as the articles offer timeless insight into the field of electrostatics.

Professor Jonassen was a member of the ESD Association from 1983-2006. He received the ESD Association *Outstanding Contribution Award* in 1989 and authored technical papers, books and technical reports. He is remembered for his contributions to the understanding of Electrostatic control, and in his memory we reprise "Mr. Static".

~ The ESD Association

When people hear about static electricity, most of them think of unpleasant shocks experienced when touching a doorknob or of electronic components being destroyed because of electrostatic discharge (ESD) events. Fifty years ago, it was more likely that static electricity would be connected with explosions in chemical or pharmaceutical factories or laboratories. However, in most cases, ESD phenomena are thought of as the result of human activity. People often overlook atmospheric electricity, which by its nature is very similar to well-known static electric processes.

If a properly grounded fieldmeter is brought outside and directed upward, the meter would likely measure an electric field directed downward with a strength of approximately 150 $V{\cdot}m^{-1}$. If the measurement were made on a mountaintop, the field may be 10 or more times stronger. These measurements are indicative of fair-weather conditions.

If there is a thundercloud overhead, the field is usually reversed and runs easily into the tens of $kV{\cdot}m^{-1}$. If a horizontal metal plate exposed to the free atmosphere is connected to ground through a sensitive ammeter, it would measure a current of about $3{\cdot}10^{-12}$ $A{\cdot}m^{-2}$. A value of 3 $pA{\cdot}m^{-2}$ is not much, but when it is taken for the earth as a whole, the current amounts to about 1500 A.

Although there are still many atmospheric electric processes that are not understood in detail, there is a general understanding of the atmospheric electric circuit (Figure 1 on page 24 provides a simplified picture of the processes). Fair-weather conditions are shown on the left side of the figure, where a downward electric field drives positive charges toward ground. Most of the field lines start at positive charges in the lower atmosphere, and some extend all the way to the atmospheric electric exchange layer (at a height of about

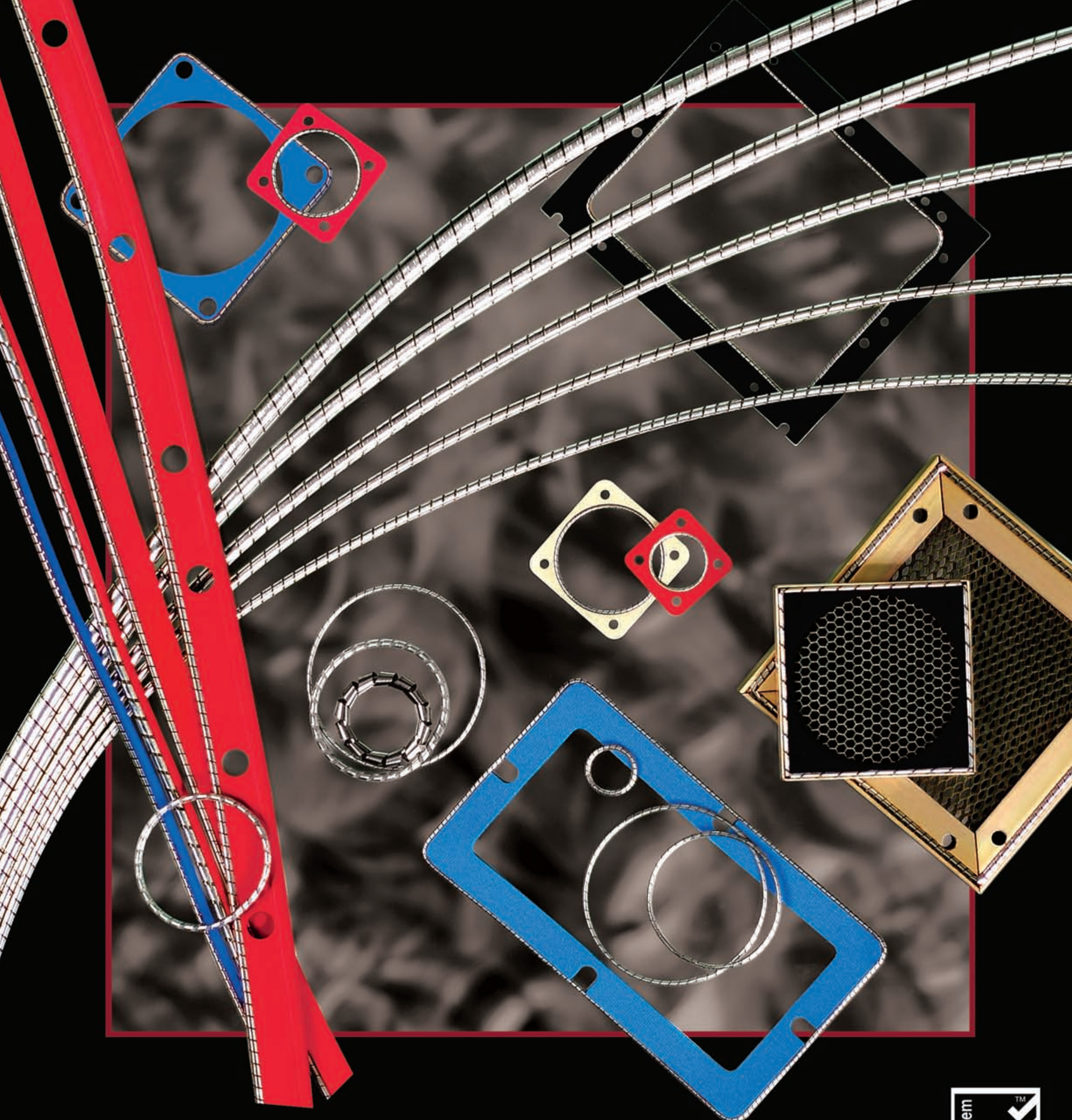

60 km), the lower part of the ionosphere. The necessary field distribution is maintained by thunderstorms (or thunderclouds), shown on the right side of the figure. A thundercloud normally has a negative base and a positive top, which brings negative charges to ground.

Furthermore, the values of the fields below the thunderclouds may be much greater than the fair-weather values, often 5–10 kV·m^{-1} as compared with a fair-weather field of 100–200 V·m^{-1}. The greater field strength may cause corona and brush discharges from the tips of leaves and branches, not to mention lightning rods, which contribute to the total current. Regular lightning discharges also represent a certain current to the ground (primarily negative), but this contribution is rather modest. The field has the same direction above, as well as below, the thunderclouds, causing a positive current to flow to the atmospheric electric exchange layer and closing the circuit (see Figure 2 for an equivalent diagram).

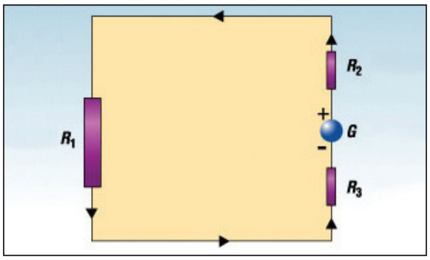

Figure 2: An equivalent diagram of the atmospheric electirc circuit

Between the exchange layer and the ground, there is a voltage difference of about 300 kV, which drives a current of about 1500 A to ground, where it is distributed over all areas with fair-weather conditions. This corresponds to a resistance R_1 of 200 W, representing the parallel resistance of all fair-weather air columns. G represents the generator effect of all simultaneously active thunder systems, and R_2 and R_3 represent the resistances of the air columns above and below these systems, respectively.

CHARGE CARRIERS

For a current to flow in a given medium, an electric field has to be established and the medium must contain mobile charge carriers. In atmospheric air, the charge carriers are air ions (or atmospheric ions), molecular clusters that carry an electric charge.

An ion is formed when a neutral oxygen or nitrogen molecule receives enough energy to lose an electron and is left as a singly positively charged elementary ion. Within less than a microsecond, the electron will combine with (usually) an oxygen molecule, forming a negatively charged elementary ion.[1] Other types of elementary ions include hydroxonium (H_3O+) and charged nitrogen oxides.

Small Ions. By polarization, both polarities of elementary ions will bind 10–20 molecules of water around themselves (a few more for positive than for negative ions) within a fraction of a second, thereby forming small molecular clusters. These molecular clusters are called air ions, and they are almost 100% responsible for charge neutralization by air ions.[2]

Large Ions. However, any atmosphere will contain aerosol particles or condensation nuclei in numbers from a few thousand to several hundred thousand per cubic centimeter. These

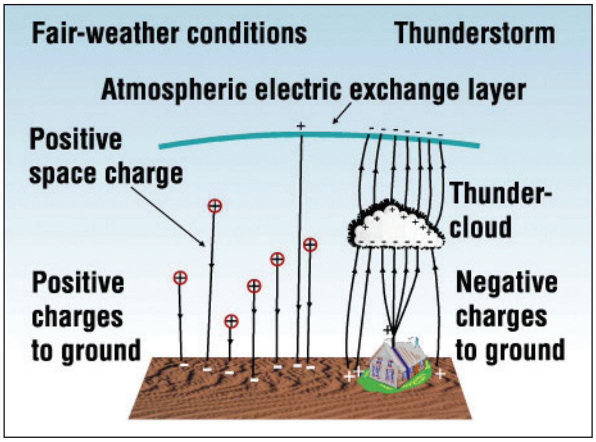

Figure 1: The atmospheric electric circuit

are particles or molecular clusters with radii ranging from 10^{-10} to 10^{-7} m. If a small ion collides with a condensation nucleus, the two may attach to form a large ion.

ION SOURCES

An air molecule may receive the necessary ionization energy from a colliding atomic particle or from a quantum of electromagnetic radiation energy. In the lower atmosphere, ions are predominantly produced by radiation from radioactive materials in the soil, in building materials, and, first of all, in the air (radon and its daughter products). Although all three types (alpha, beta, and gamma) of radiation may ionize the air, alpha radiation is by far the most important.

An alpha particle (with energies in the order of 4–8 MeV [6–13 x 10^{-13} J]) emitted from a decaying radioactive atom (see Figure 3) will, along its trajectory through the surrounding air, knock off electrons from oxygen and nitrogen molecules—at the expense of about 34 eV per successful collision. Cosmic radiation contributes maybe 10% to the ionization at ground level. However, at higher altitudes, the partitioning shifts dramatically both because the radiation from the soil and airborne materials decreases and because the intensity of the cosmic radiation increases.

MOBILITY

Normally, ions are characterized by their mobilities. If an ion is exposed to an electric field *E*, it will move with a constant velocity *v* given by:

$$v = kE. \tag{1}$$

For positive ions, *v* is in the direction of the field, and for negative ions, *v* is in the opposite direction.

The factor of proportionality, *k*, represents the mobility of the ion. The unit of *k* is (m/second)/(V/m) = $m^2 \cdot V^{-1} \cdot s^{-1}$. Small positive ions have mobilities of approximately 1.4 x 10^{-4} $m^2 \cdot V^{-1} \cdot s^{-1}$, and small negative ions have about 1.8 x 10^{-4} $m^2 \cdot V^{-1} \cdot s^{-1}$. The difference in mobility reflects the difference in the numbers of attached water molecules in the ions. Large ions cover a range of mobilities from about 3 x 10^{-7} to 8 x 10^{-8} $m^2 \cdot V^{-1} \cdot s^{-1}$, depending partially on the nature and size distribution of the aerosol particles in the air.

REMOVAL PROCESSES

An ion has a limited lifetime. It may deposit on a surface either by diffusion or by the aid of an electric field. An ion may combine with oppositely charged ions or particles and hence cease to exist as an ion, or with aerosol particles and then either be neutralized or become a large ion. This latter process usually determines the lifetime of an ion. In polluted city air, the average lifetime

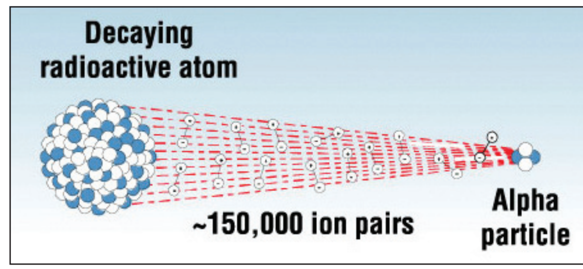

Figure 3: A decaying radioactive atom emitting an alpha particle

It has been known for more than two centuries that the normal prevailing condition in the atmosphere is best described in today's language as an electric field directed downward, bringing a positive charge to the ground.

may be in the order of 10–20 seconds, whereas in polar air, poor in aerosols, the lifetime may be as long as 300–400 seconds.

CONDUCTIVITY

For a current to flow in a medium, that medium must contain mobile charge carriers. Consider an atmosphere containing one type of ions with the concentration n and the mobility k, with each ion carrying a single elementary charge e. If an electric field E is established in the medium, a current with the density j will flow in the medium in the direction of the field (for positive ions) given by $j = enkE$ or

$$j = \gamma E. \qquad (2)$$

Equation 2 is Ohm's law in differential form. The factor

$$\gamma = enk \qquad (3)$$

is called the conductivity of the air, and the unit is $W^{-1}\cdot m^{-1}$.

It appears from Equation 3 that, of two groups of ions with the same concentration, the group with the greatest mobility contributes the most to the conductivity. It is often convenient to separate the contributions to the conductivity of positive and negative ions by introducing the polar conductivities, that is, the conductivities caused by the positive and negative ions, separately. In the case of an atmosphere with the concentration n^+ and mobility k^+ for positive ions and n^- and k^- for negative ions, the polar conductivities are $g^+ = en^+k^+$ and $g^- = en^-k^-$. Both polar conductivities are positive quantities, causing positive currents to flow in the direction of the field, with positive and negative charge carriers moving in opposite directions.

Usually, the ions do not all have the same mobility but are, in general terms, distributed according to some function of frequency $f(k)$ in such a way that the concentration dn of ions with mobilities from k to $k + dk$ is given by $dn = f(k)dk$. The conductivity may then be written as

$$\gamma = e\int_0^\infty kf(k)dk. \qquad (4)$$

Normally, only small ions contribute significantly to the conductivity of the air because their mobility is much greater than that of large ions and charged particles.

At ground level, under fair-weather conditions, the average value of the conductivity is about 2 x 10^{-14} $W^{-1}\cdot m^{-1}$. The conductivity shows annual and diurnal variations, depending on variations in the ionization and aerosol conditions. The conductivity increases with increasing altitude both because of the decrease in aerosol concentration and because of the increase in the cosmic radiation intensity. At an altitude of 5 km, the conductivity may be about 10 times greater than at ground level.

THE VERTICAL FIELD

It has been known for more than two centuries that the normal prevailing condition in the atmosphere is best described in today's language as an electric field directed downward, bringing a positive charge to the ground. At ground level, the field strength is about 100–150 $V\cdot m^{-1}$. The field strength decreases rapidly with increasing altitude, and at 5 km, the field strength is about one-tenth of the value at ground level.

The potential of the atmosphere can be found by integrating the field strength with respect to height. At a height of approximately 60 km, the field strength is virtually zero, and, consequently, the potential does not change with further increases in height. This is the location of the atmospheric electric exchange layer shown in Figure 1. The mean value of the potential of the exchange layer is about 300 kV.

The current density (see Equation 2) is more or less constant in a given vertical column of air and can be written as

$$j = \gamma E = \frac{V}{R_c}, \qquad (5)$$

where V is the potential of the

atmospheric electric exchange layer and R_c is the columnar resistance (i.e., the resistance of an air column that extends from the ground to the exchange layer and has a unit area cross section).

Equation 5 expresses two important relations. For a given value of V, the conductivity g and the field strength E are inversely proportional, which is in good accordance with experiments. For locations where the conductivity exhibits small changes with time (e.g., over the oceans), the field strength is, at a given place, proportional to the potential of the exchange layer, and recordings of the field strength may therefore reveal patterns in the value of this potential.

The top graph of Figure 4 shows an example of an atmospheric field strength recording, normalized to the mean value, as a function of Greenwich mean time (GMT). It appears that the field strength, and therefore the exchange layer potential, has a minimum at 3 GMT and a maximum at 19 GMT.

Because the atmospheric field and potential are maintained by active thunderstorms, it is therefore to be expected that variations in the field and potential reflect corresponding variations in concurrent thunderstorm activity. Such a relationship is shown in the bottom graph of Figure 4. The graph plots areas where, at a given time, thunderstorms are active in major parts of the world. A place is regarded as having been in a thunder area at a specified time if thunder was audible in the interval from 60 minutes before to 60 minutes after that time. Although this is a rather uncertain estimate, the curve for the world as a whole does show a correspondence with the field strength curve plotted in the top graph, allowing a causal relationship to be deduced.

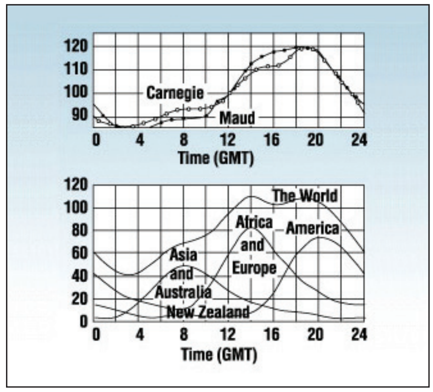

Figure 4: Example recordings of field strength as a function of Greenwich mean time

ATMOSPHERIC CURRENTS

The effect of the ground-level field strength of 150 $V \cdot m^{-1}$ and conductivity of 2 x 10^{-14} $W^{-1} \cdot m^{-1}$ is, according to Equation 2, a current to the ground with the density *j* @ 3 x 10^{-12} $A \cdot m^{-2}$. This is the fair-weather vertical current density, but this field-induced charge transport is not the only way by which charge is brought to the ground.

It has long been known that most precipitation elements, such as rain drops, snowflakes, and hailstones, are often charged. If large raindrops are falling in a strong turbulent updraft, they may split into smaller droplets. The majority of the smallest droplets are negatively charged because of the Lenard effect, that is, the breakup of the electrical double layer at a water-air interface.

A similar process may charge snow particles, but it should be mentioned that charging processes are much more complicated with solid materials. The charging involves contact and friction, and the result therefore depends on the physical state of the contacting materials (temperature, purity, origin, etc.). For example, it has been shown that when two ice pellets are rubbed against each other, the ice pellet with the higher conductivity will become negative, regardless of whether the higher conductivity is caused by higher temperature or lower purity.
The charge brought to the ground by precipitation is normally positive, averaging about 30 C/km^2 per year, or about 10^{-12} $A \cdot m^{-2}$. The charge from precipi-tation together with the fair-weather vertical current yields a positive current to the ground of about 4 x 10^{-12} $A \cdot m^{-2}$, or a total current of about 2000 A to the earth as a whole.

The second part of this article on atmospheric electricity will show that the collective effects of thunderstorms are enough to balance the current brought to the ground. In addition, the physics of lightning discharges will be discussed.

REFERENCES

1. Niels Jonassen, "Ions" in Mr. Static, *Compliance Engineering* 16, no. 3 (1999): 24–28.
2. Niels Jonassen, "Neutralization of Static Charges by Air Ions: Part I, Theory" in Mr. Static, *Compliance Engineering* 19, no. 2 (2002): 28–31.

(the author)

NIELS JONASSEN, MSC, DSC,

worked for 40 years at the Technical University of Denmark, where he conducted classes in electromagnetism, static and atmospheric electricity, airborne radioactivity, and indoor climate. After retiring, he divided his time among the laboratory, his home, and Thailand, writing on static electricity topics and pursuing cooking classes. Mr. Jonassen passed away in 2006.

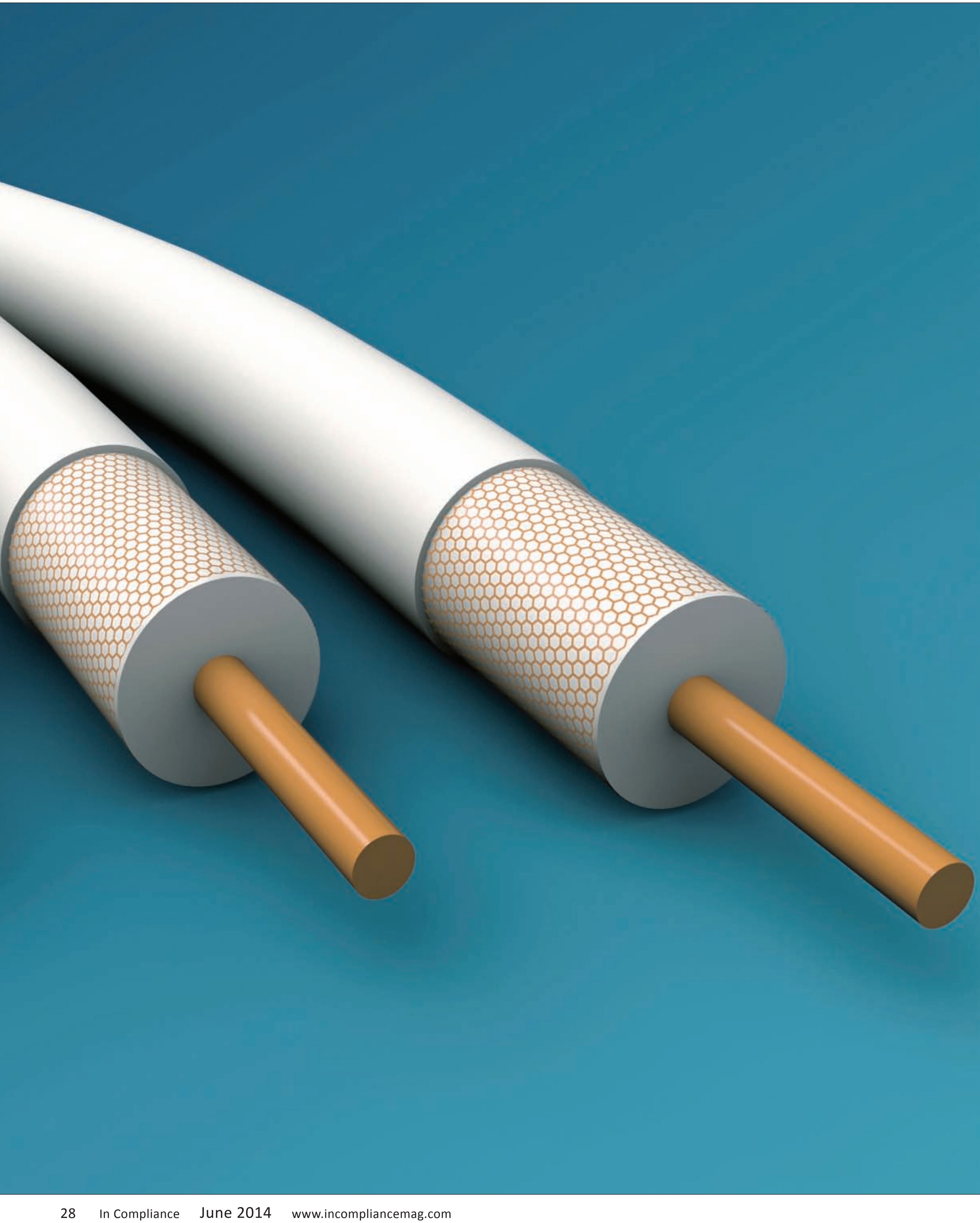

Things You May Not Have Heard About Shielding

BY AL MARTIN

What determines how effective a cable shield is going to be? And how does the decision to ground or not ground a shield impact its effectiveness?

Fortunately there is a well-developed theory of shielding, which will be discussed as a way to get a general understanding of what can be expected of shield performance. But there's more to it. The manner in which the shield is terminated can significantly affect its effectiveness, as we shall see.

THE THEORY OF SHIELDING

A model of the physical environment

The theory of shielding starts with a model of the physical environment of the shield. The model assumes that the cable is jacketed, so that a shield is not in contact with a ground plane anywhere except possibly at the ends. That being the case, a transmission line is formed by whatever ground plane exists and the outside of the shield. Likewise the inside of the shield and the conductors enclosed also form a transmission line. Thus what we have is two transmission lines coupled by the leakage through the shield (see Figure 1).

The coupling of the inner and outer transmission lines is characterized by a mechanism called surface transfer impedance, Z_t. In most installations the shield, and hence the outer transmission line, is shorted to ground either at both ends or one end, shown schematically in Figure 2 (page 30), by the switch SW being closed or open respectively.

The inner conductors are terminated at each end in some impedance, which when measurements are done, is generally an open, short or matched load.

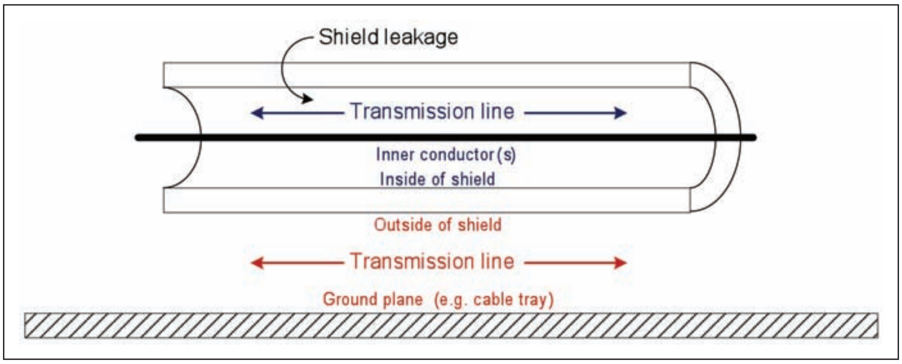

Figure 1: The basic model of the physical environment

A model of the electrical environment

If the shield is terminated at both ends, current can flow along the outside of the shield. This current can be due either to ground loops caused by the grounds at the ends of the cable being at different potentials (V_d), or it can be due to induction from external fields, or both. In either case the external shield current is coupled into the inner circuits via the surface transfer impedance, Z_t.

If the shield is terminated at only one end, the ground loop is broken. Current is limited to that which is induced to flow through the distributed capacitance between the outside of the shield and the ground plane (see Figure 3).

The induced current may be small, in which case the important quantity is the voltage distribution along the cable. The voltage is zero where the cable is terminated, but can be high at the open end for frequencies where the cable exceeds one-tenth of a wavelength, because, at that point, it becomes a very efficient antenna.

At the open end, there is capacitive coupling between the shield and the conductors of the cable due to the fringing capacitance C_f (see Figure 4). As the voltage across this capacitance can be high, a significant current can be coupled into the conductors of the cable through the fringing capacitance.

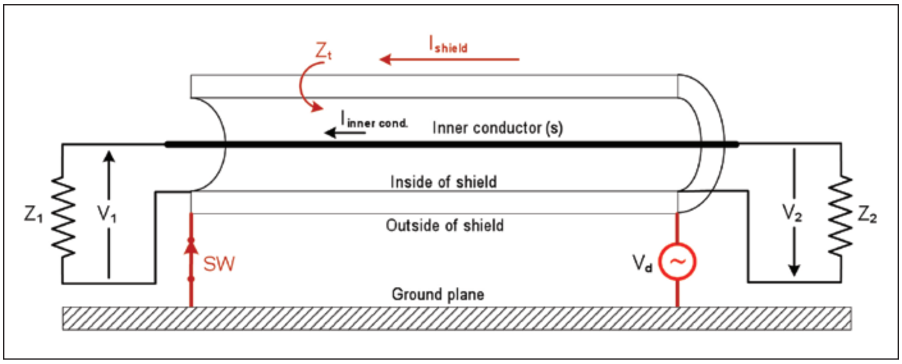

Figure 2: The model of the physical environment including terminations

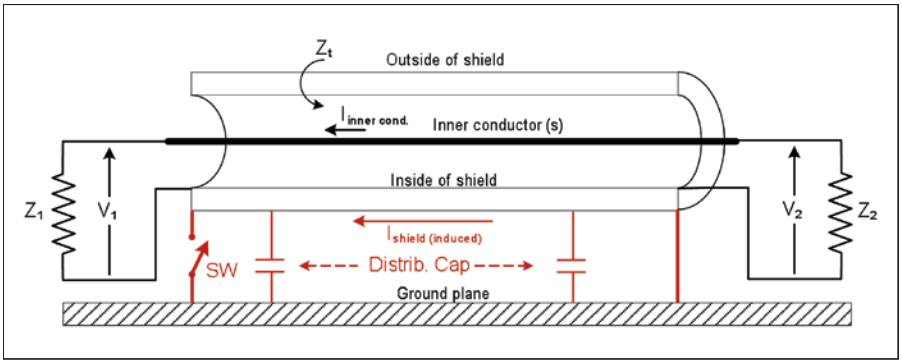

Figure 3: Model of a cable terminated at only one end

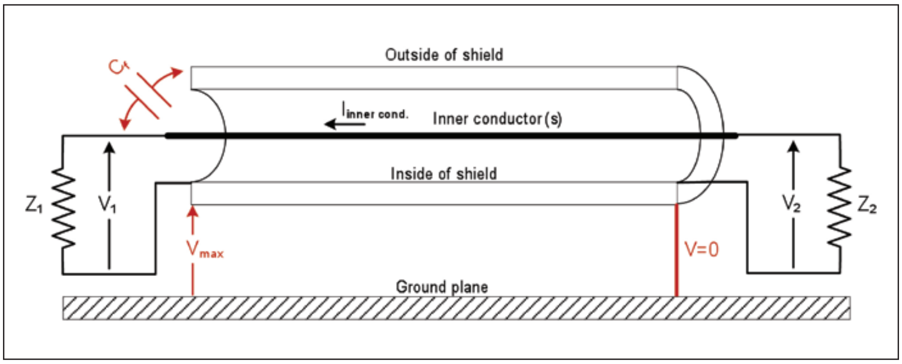

Figure 4: The basic schematic for coupling when one end of the shield is open-circuited

So far we have considered a model of the physical and electrical environment of a shield. Now we need to consider the characteristics of a shield's construction, and how that impacts shield performance.

Surface transfer impedance

To begin with, let's consider a cable grounded at both ends. To see how a cable grounded in that way works, we need to discuss surface transfer impedance. Simply stated, surface transfer impedance relates the voltage developed across circuits inside a shielded cable to currents flowing on the outside of the cable. Thus in Figure 2 with the switch closed, the current I_{shield} on the outside of the shield gives rise to V_1 and V_2 on the conductors inside the shield, via Z_t.

So how do we determine what Z_t is? Well, we can measure it, or we can calculate it. The measurement route has been described in [3], and an example will be shown later. The calculation route is worth discussing because it provides an insight to the physics involved.

We said earlier that the cable shield and the ground plane form a transmission line. We cannot say much about the general case of this, so for simplicity we'll consider a coax with a ground plane wrapped around it, as shown in Figure 5.

In this case, the shield and the ground plane form a coax (so we have a coax within a coax, often called a triax). This configuration can be achieved in practice for a jacketed shielded cable by pulling a braid over the jacket; which is often done for measuring Z_t, as explained in [4].

Now let's suppose a current is flowing along the outside of the shield. From Maxwell's equations, this current will generate a travelling wave which has electric and magnetic fields, as illustrated in Figure 6. If the conductors have no resistance, the E-field (E_r) is radial, and the H-field (H_Θ) is circumferential (the TEM mode that some of you may be familiar with). However, since the shield has some resistance, the product of the current flowing on the shield and the shield resistance will generate an E-field E_Z in the Z direction, so that the resultant E-field is no longer radial but "tipped" as shown in Figure 7.

Because the shield has a finite resistance, the E_Z field does not vanish in the shield, but has a strongly decaying value as a function of the penetration depth (related to the concept of "skin depth"), shown schematically in Figure 8. The E_Z wave reaches some (greatly attenuated value) $E_Z(a)$ on the inside of the shield.

From circuit theory, $E_Z(a)$ is related to $E_Z(b)$ by the relations:

$$E_Z(a) = Z_{aa}I_a + Z_tI_b$$

$$E_Z(b) = Z_tI_a + Z_{bb}I_b$$

Where I_a is the current on the inside of the shield, I_b is the current on the outside of the shield, Z_{aa} is the surface impedance of the shield inside, and Z_{bb} is the surface impedance of the shield outside. Z_{aa}, Z_{bb} and Z_t can be calculated from the physical properties of the case, e.g. Schelkunoff [1].

Rearranging the equations on the previous slide, the $E_Z(a)$ field at the

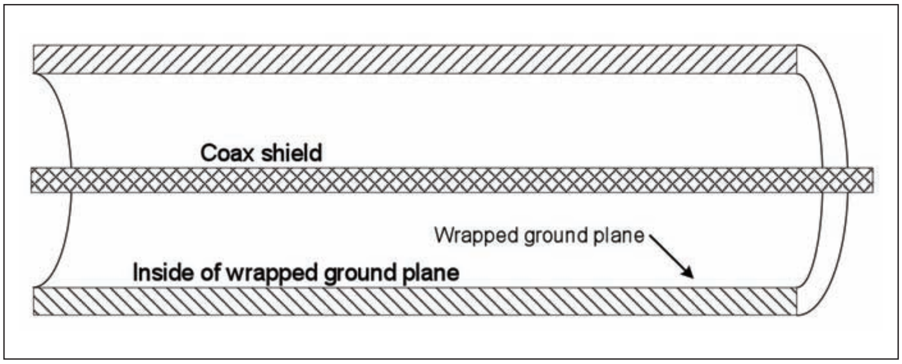

Figure 5: Basic configuration for calculating Z_t

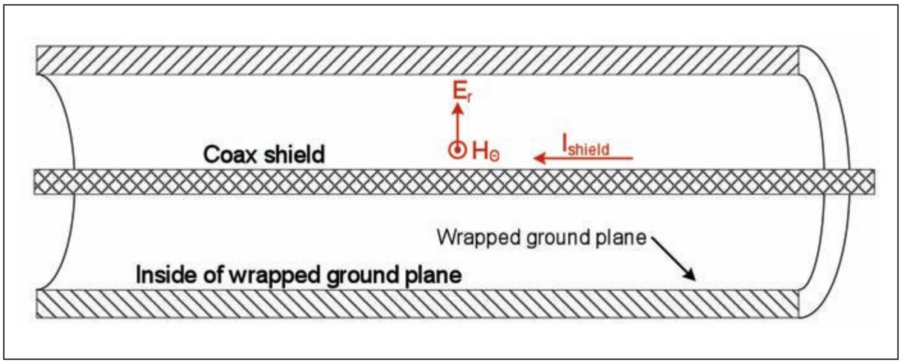

Figure 6: Shows the fields of the travelling wave

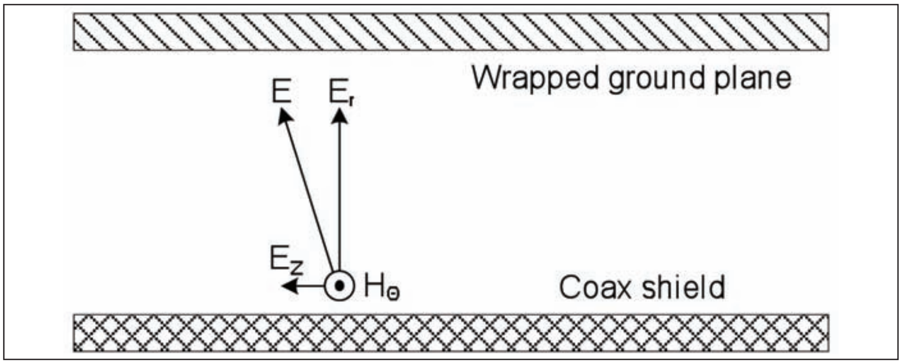

Figure 7: Orientation of the fields for calculating Z_t

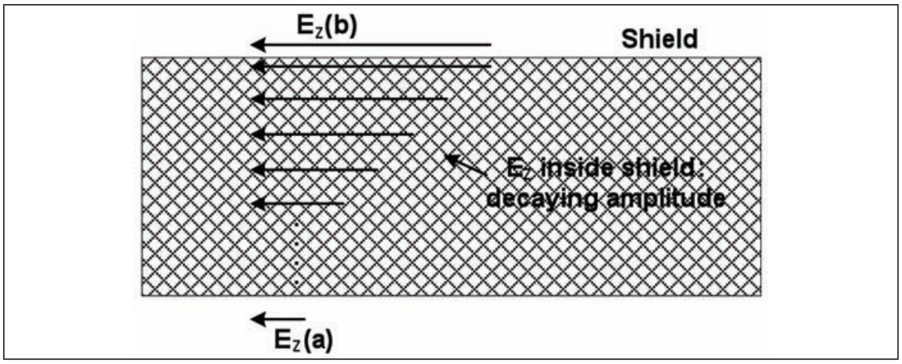

Figure 8: A wave with an $E_Z(b)$ component travelling on the outside of a shield, having a decaying component in the shield, reaching $E_Z(a)$ inside the shield

Braided shields behave differently from solid ones, due to the holes in the shield created during the braiding process. The situation is similar for wrapped shields, which look like slot antennas.

inside of the shield can be expressed in terms of the current I_b and voltage $E_Z(b)$ at the outside of the shield as:

$$E_Z(a) = \frac{Z_{aa}}{Z_t} E_Z(b) + \left[\frac{Z_t^2 - Z_{aa}Z_{bb}}{Z_t}\right] I_b$$

Ignoring the terms that are small

$$E_Z(a) = Z_t I_b$$

The calculation route for Z_t: Solid shields

A formula for calculating Z_t was given by Shelkunoff as

$$Z_t = \frac{UR_{DC}}{\sqrt{\cosh U - \cos U}}$$

$$U = 303t\sqrt{\mu_r \sigma_r f}$$

where R_{DC} is the dc resistance of the shield, t is the thickness of the shield in centimeters, μ_r is the permeability of the shield relative to air, σ_r is the conductivity of the shield relative to copper, and f is the frequency in megahertz. Notice that Z_t depends on frequency.

Inside the shield, $E_Z(a)$ drives a, basically, TEM wave (if the conductor resistance is small) that propagates along the conductors. The current I_a caused by the wave that travels inside the shield gives rise to voltages V_1 and V_2 across the terminations of the cable (see Figure 2). The amplitude of the current [and hence V1 and V2] depends on $E_Z(a)$ and Z_t.

To see whether Shelkunoff's formula actually works, we made a measurement on RG402, a solid-shield coax [3]. The results are shown in Figure 9, where the terms short-short and short-matched refer to two different methods of measuring surface transfer impedance. Figure 9 shows that Shelkunoff's formula is a good predictor of surface transfer impedance [and hence shielding effectiveness]. It also shows that, for a solid shield, shielding effectiveness keeps getting better as frequency increases.

The measurement route for Z_t: Cables with braided (wrapped) shields

Braided shields behave differently from solid ones, due to the holes in the shield created during the braiding process. The situation is similar for wrapped shields, which look like slot antennas. The holes or slot couple the fields outside the shield to the fields inside the shield by mutual inductance and capacitance. Surface transfer impedance can be calculated for this case, *e.g.* see [2]. But it's messy, in particular because it is hard to determine what the mutual capacitance and inductance are.

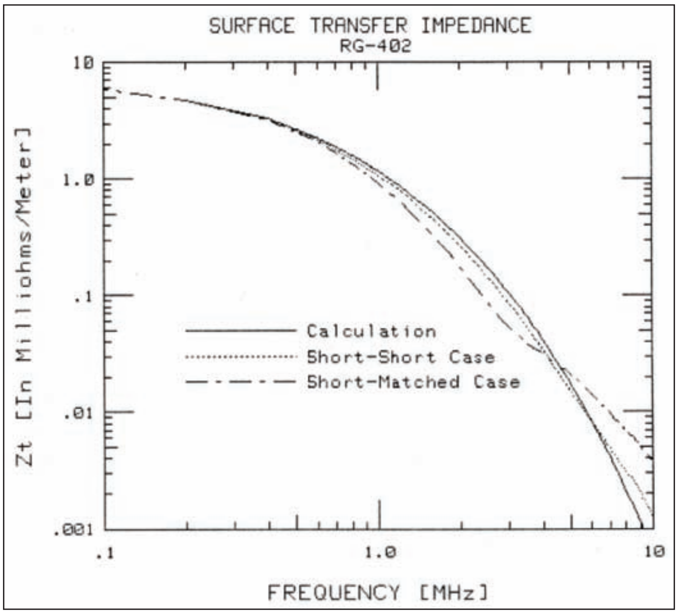

Figure 9: Example of Z_t for a solid shield

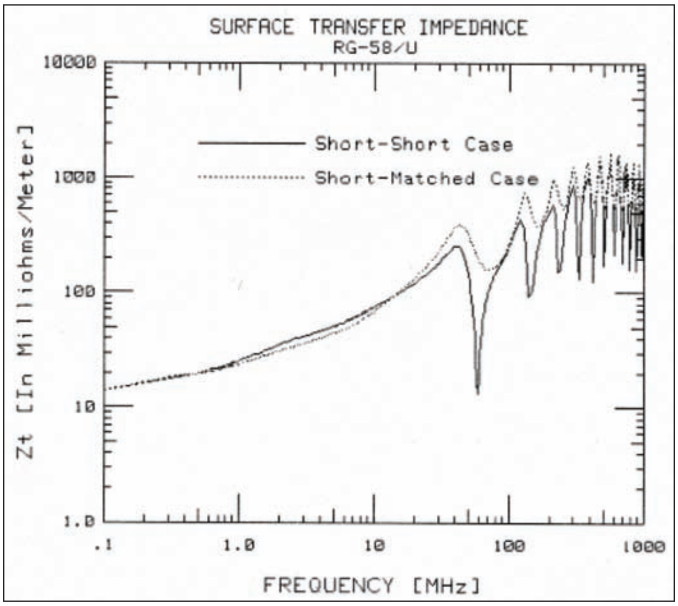

Figure 10: Example of Z_t for a braided shield

Regardless of how the braided or wrapped cable shield is terminated, it basically acts like a high-pass filter. The result is that a surge travelling on the inner conductors of a shielded cable will have a steeper rise-time than the inducing surge on the outside of the shield.

Generally what is done is to produce a sample of the braided or wrapped cable, and then measure its Z_t as a function of frequency (as a measure of shielding effectiveness). As an example, using a method developed to do this [3], we measured the Z_t of RG-58U, a widely used coaxial cable. The result is shown in Figure 10. Notice that, in contrast to solid shields, Z_t for a braided shield increases with frequency, and eventually becomes oscillatory. Wrapped shields in general show the same behavior as braided ones.

An important point, as explained in [5], is that Z_t increases to a first peak value as frequency is increased, and this peak is never exceeded as frequency is further increased. The frequency at which the first peak occurs depends on the length of the cable, and moves to lower frequencies as cable length increases. Indeed Z_t can be plotted against the product of frequency and cable length. For example, a plot like the one in Figure 11 can be generated by fitting a curve to the peak values of the data plotted in Figure 10.

Why this happens is explored further in [5] and [4], where the oscillatory behavior as a function of the length of the cable and frequency is discussed; and also why Z_t reaches a peak value at some frequency, and then decreases as frequency is further increased.

EFFECT OF A SHIELD ON WAVESHAPE

Regardless of how the braided or wrapped cable shield is terminated, it basically acts like a high-pass filter. The result is that a surge travelling on the inner conductors of a shielded cable will have a steeper rise-time than the inducing surge on the outside of the shield. As an illustration, the effect of a shield grounded at both ends on the frequency spectrum of a lightning surge is shown in Figure 12. Here the frequency spectrum of a 4.5x77 negative first lightning surge has been

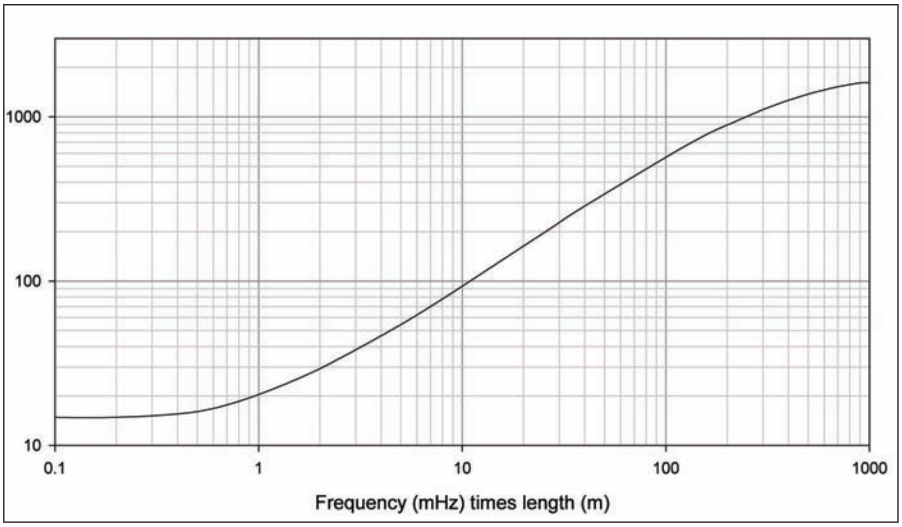

Figure 11: Z_t from Figure 10 plotted as the product of frequency and cable length

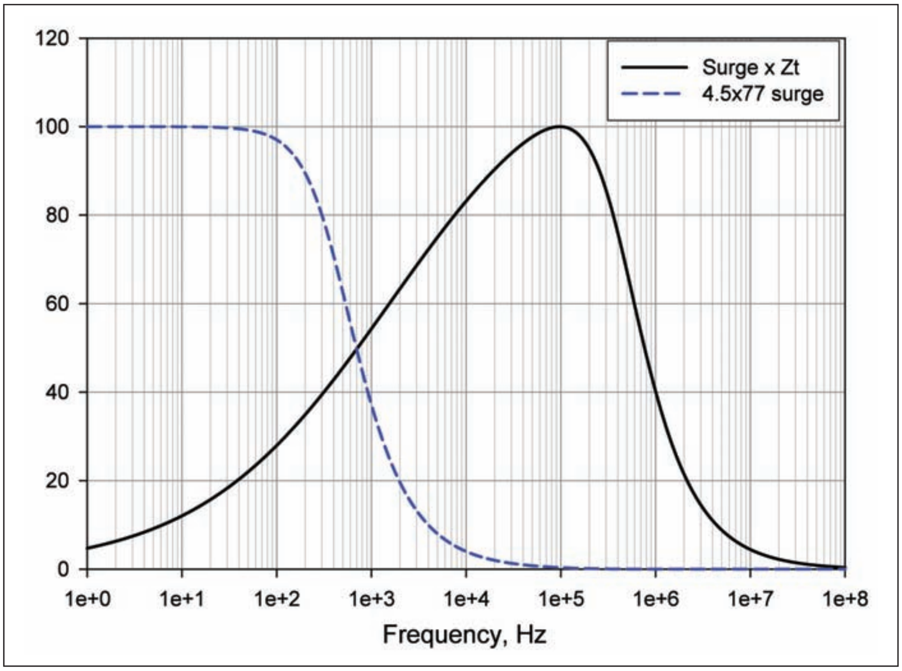

Figure 12: The effect of a 10 m RG-58 coax shield grounded at both ends on a 4.5x77 negative first lightning surge

multiplied by the Z_t spectrum shown in Figure 11, assuming a 10 m long cable. Figure 12 shows that the low-frequency components of the surge are suppressed. The result is that the surge appearing on the inner conductors of the cable will have a steeper rise time than the surge on the outside of the shield. Note that a similar effect would occur if the shield were grounded at only one end, since the resulting capacitive coupling also suppresses the low-frequency components of the surge.

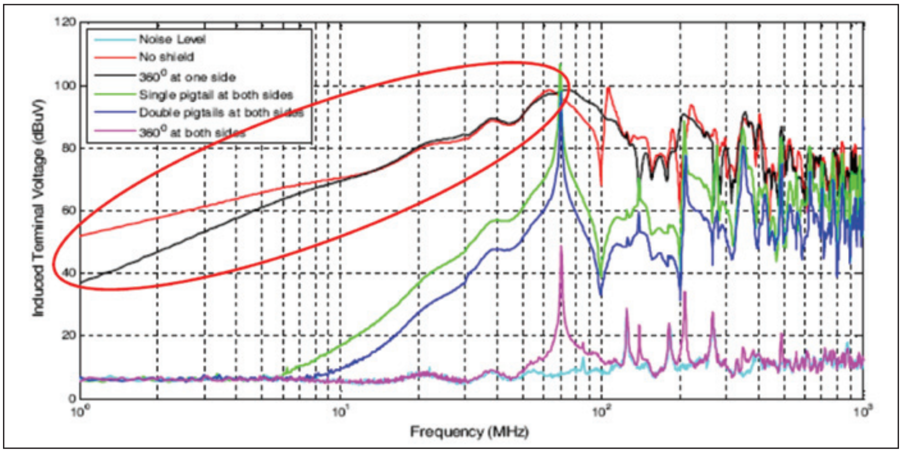

Figure 13: The effect of terminating a shield at only one end

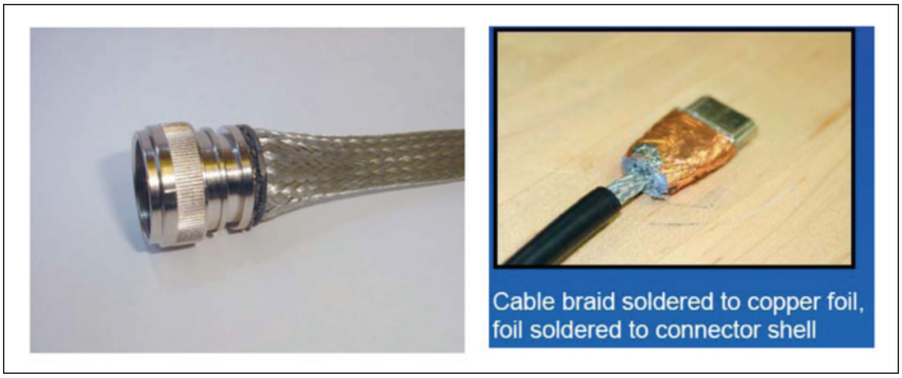

Figure 14: Two examples of 360° shield termination

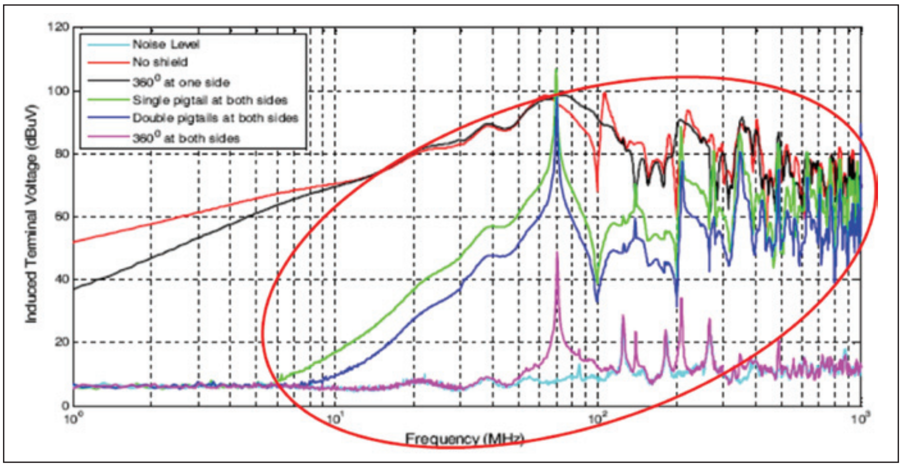

Figure 15: Loss of shielding effectiveness due to terminating the shield with pigtails

THE EFFECT OF SHIELD TERMINATION

Having looked at shielding theory, there is the practical matter of how to terminate the shield. This decision depends on the environment in which the cable is installed.

If a shield is terminated at only one end, a relatively high voltage may exist at the open end of the shield. Because a capacitance exists between the end of the shield and the cable conductors, electrical interference can be injected directly into the cable loads. The magnitude of this capacitance depends a lot on the installation, so it cannot really be calculated. The capacitive coupling is greatest at high frequencies, where the capacitive reactance is the lowest.

The argument has been made [6] that bonding a shield at only one end destroys its effectiveness, and there is some truth to it, especially at high frequencies, as shown in Figure 13 based on data in [7]. The implication of that remark is that a shield should never be bonded at one end only. But the remark was made in the context of saying that a properly designed system does not have ground loops – a condition that may not be achievable in practice.

As a note, the difference between the “no shield” and the “360° at one side” plots in Figure 13 is 18 dB at 1 mHz. Extrapolating this plot to 100 Hz [a pretty risky thin to do] leads to an estimated difference between the two curves of 63 dB. So a shield grounded at only one end may have reasonable performance at audio frequencies, but not at broadcast radio frequencies and higher.

Grounding a shield at both ends eliminates the capacitive coupling problem and is most effective when the potential difference between the

An important factor to consider is whether or not the grounds at opposite ends of the cable are at close to the same potential. If they are, ground-loop currents will be minimal.

two shield terminations is low. In this case, the ground loop currents will be small, and the shield will have its maximum effectiveness, provided it is terminated properly. As pointed out in [6], proper termination is for the shield to be bonded at each end with a 360° termination. Figure 14 shows two examples.

If that is not done, much of the benefit of terminating a shield at both ends may be diminished or lost; for example, as shown in Figure 15 from data in [7]. Note the loss of shielding effectiveness when pigtails are used (see also [8]).

CONCLUSIONS

Back to the original questions: What determines how effective a cable shield is going to be? And how does the decision to ground or not ground a shield impact its effectiveness?

The theory of shielding gives a general understanding of what can be expected of shield performance, but the manner in which the shield is terminated also has a significant impact on the effectiveness of the shield.

An important factor to consider is whether or not the grounds at opposite ends of the cable are at close to the same potential. If they are, ground-loop currents will be minimal. In this case grounding both ends of the shield is likely to give the best shielding performance. If the grounds are at substantially different potentials, ground-loop currents could be a problem, and in this case leaving one end of the shield unterminated may give the best overall shielding performance, providing that shielding against high frequencies is not an issue.

The decision to terminate or not terminate depends on the application. Unfortunately, there is no rule that applies to all situations, and an experiment is often required to determine the best way to terminate the shield.

REFERENCES

1. Shelkunoff, S.A. "The Electromagnetic Theory of Coaxial Transmission Lines and Cylindrical Shields." *Bell Syst. Tech. J.* 13 (October 1934): 532-579.
2. Merewether, D.E. and T.F. Ezell. "The Effect of Mutual Inductance and Mutual Capacitance on the Transient Response of Braided-Shield Coaxial Cables." *IEEE Trans. on EMC,* EMC-18 (February 1976): 15-20.
3. Martin, A.R. and M. D. Mendenhall. "A Fast, Accurate and Sensitive Method for Measuring Surface Transfer Impedance," *IEEE Trans. on EMC,* EMC-26 (1984): 66-70.
4. Martin, A.R., and S.E. Emert. "Shielding Effectiveness of Long Cables." *IEEE International Symposium on EMC*, San Diego (1979): 13-18.
5. Martin, A.R., "The Shielding Effectiveness of Long Cables, III: Maximum Leakage," 5th Symposium and Technical Exhibition on EMC, Zurich, Edited by T. Dvorak. (1983): 379-84.
6. Waldron, Tony and Keith Armstrong. "Bonding Cable Shields at Both Ends to Reduce Noise." www.compliance-club.com/archive/old_archive/020514.htm.
7. Üstüner, F., N. Tarim, and E. Baran. "Experimental Investigation of the Shield Termination Effect on the Field-to-Cable Coupling Level." *Progress in Electromagnetics Research Symposium Proceedings,* KL, Malaysia, (2012): 19-22.
8. Paul, C.R. *Introduction to Electromagnetic Compatibility*, 2nd ed. New Jersey: Wiley Interscience, 2006.

(the author)

AL MARTIN

Al holds a BEE degree from Cornell University, and a PhD from UCLA. Al joined Raychem in 1975, where he was initially involved with shielding effectiveness and surface transfer impedance measurements. Al went on to hold a number of positions with Raychem [which became TE Connectivity], retiring in 2013. Al has been a contributing member of TIA TR41, ATIS NIPP- NEP, ITU-T, the IEEE EMC Society, and the IEEE Power and Energy Society. He has been an editor for TIA TR41, ATIS NIPP-NEP, and IEEE standards, and is presently chairman of IEEE PES SPDC WG3.6.7 [Data, Communications and Signaling Circuit Surge Protective Devices], and vice-chairman of WG3.6.2 [Solid State Surge Protective Device Components]. He is the author or co-author of over 20 papers on EMC and telecommunications. Al is a Life Senior member of the IEEE and the IEEE SA.

EU-US Transatlantic Trade and Investment Partnership

Can thousands of regulations be harmonized?

BY STEPHAN SCHMITT

Last summer, the European Union (EU) and the US took the first steps to establish a partnership between the two markets that together account for almost half the world's economy. Teams of negotiators met in Washington to talk about how best to take the Transatlantic Trade and Investment Partnership (TTIP) forward, and even though the second round of negotiations was canceled due to pressing political issues, both sides expressed a firm commitment to the TTIP process.

The possibility of TTIP is important as the partnership promises both sides significant economic benefits. According to US Trade Representative (USTR) Michael Froman, trade and investment between the US and the EU currently far exceeds any other bilateral relationship, with $2.6 billion worth of goods flowing between the two sides each day. Many Americans do not realize that more than 13 million people in two countries owe their jobs to the transatlantic economic relationship.

At the time when the American and European governments are working to stimulate economic growth and job creation, regulatory inefficiencies can hardly boost their efforts. Some products have to go through two separate testing procedures even where the requirements on both sides of the Atlantic are the same, leading to vast inefficiencies in trade, and making it particularly difficult for small and medium sized enterprises to expand their markets.

The TTIP would address two areas: tariff-related trade barriers such as customs duties; and non-tariff-related trade barriers such as licensing regulations, compulsory certifications and standards. In the global economy, harmonization of standards becomes, in a way, a precondition for the free trade with a mutual recognition and eventual alignment of standards defining the traffic of goods. Greater harmonization would allow manufacturers to save costs by reducing the number of certificates and tests their products need to pass.

Should the agreement become reality, manufacturers would benefit from scalable effects. For them, the need for only one test instead of many means faster time to market and lower testing costs. These benefits will help the economy as a whole as new markets open up and various industries grow. This would also lead to growth in the testing and certification business, as there would be increased mid- to long-term development in the transatlantic economic zone. Consumers would also benefit as product prices go down and increased competition enhances product quality and selection. This article will discuss the potential of TTIP to change for the better not only the US and EU economies but also economies of their trade partners.

ECONOMIC GROWTH

GDP

The study by the Centre for Economic Policy Research (CEPR), an independent, non-profit research organization based in London, estimates that an ambitious and comprehensive TTIP could bring significant economic gains for the US ($129 billion) and the EU (about $163 billion) once the economies implement fully the agreement. These economic gains would translate into a 0.5% and 0.4% increase in the EU and US GDP respectively by 2027 as compared to their levels without TTIP. The gains will be increasing every year from the moment the agreement comes into force until it reaches its full level by 2027.

While the CEPR study is based on an advanced computable general equilibrium model to simulate the impact of TTIP and is a standard tool of trade economists, keep in mind that these are ballpark estimations, not precise predictions.

Tariffs

The CEPR study assumes that the tariff barriers be reduced to zero, non-tariff barriers in goods and services be reduced by 25% and public procurement barriers reduced by 50%. The assumptions are based on the commitment expressed by both parties: Office of the USTR announced that the TTIP would eliminate all tariffs on trade as well as tackle costly "behind the border" non-tariff barriers that impede the flow of goods. Reducing non-tariff barriers is a crucial driver of the economic gains. According to the CERT analysis, as much as 80% of the total potential gains could come from reducing costs imposed by duplicative bureaucracy.

Companies would benefit from more variety and lower prices for the parts, components and services that they use in their business. As a result, they would be better able to compete on their home markets and around the world.

Consumer

Increases in GDP translate into a permanent increase in wealth for more than 800 million people on both sides of the Atlantic. The CEPR study found that the TIPP would have a positive impact both on skilled and less skilled workers' wages, raising each by about the same amount, roughly 0.5%. The assumption is that the industries growing thanks to the TTIP would be able to offer higher wages to attract employees.

As with any trade deal, both imports and exports would increase, giving consumers more choices at lower prices. It is estimated that the average American family of four will see an increase in disposable income of $865 annually, with its European counterpart adding about $720. This figure accounts for both an increase in wages and price reductions.

THE CASCADING EFFECT OF TTIP

The TTIP benefits are not limited to the US and Europe but extend to their trading partners around the world by the estimated $137 (€99) billion. Predicted economic growth of the two powerful economies, coupled with an increase in the household income, will allow consumers and businesses to purchase more products, made both domestically and abroad.

Any joint regulatory approaches or streamlined certifications between the EU and the US will reduce costs for manufacturers trading in these markets. Eliminating or reducing regulatory barriers will allow for improved market access for manufacturers from other countries. Many companies around the world that export to both Europe and the States currently have to comply with two sets of standards and regulations, often requiring separate production processes. Two specific examples are the IT and automotive industries, which are highly bound to regional standards and must go, at times, through duplicate tests for each region.

Moreover, one needs to keep in mind the highly interdependent nature of the world economy, with complex global value chains. As American or European companies produce more products, the demand for components and services from their suppliers in other countries will also increase.

STANDARD-SETTING PREROGATIVE

World-class safety and quality standards are indispensable for successful economies. Competent and rigorous certification builds confidence in products and brands in developed and emerging markets. The economic powers of the US and EU have a strong bearing on the emerging international standards. Their combined influence in bodies such as the American National Standards Institute and Deutsches Institut für Normung (DIN), or the German Institute for Standardization, affords them the potential to create a universally acceptable set of regulatory practices that could be adopted internationally. Manufacturers and suppliers from outside the TTIP economic zone will have an incentive to move towards product standards agreed between the Europe and America. This would improve market access between the EU, US and their third-party partners, and may even reduce trade barriers among those countries themselves.

Many independent testing and certification bodies are working now to make sure that future negotiations succeed in making the world a safer place.

While sophistication and expertise of the two developed regions positions them to lead in the standard setting area, they must not take this position for granted. With so much manufacturing focused in China, and the emergence of premium brands such as Huawei and Lenovo, the US and EU risk gradually losing influence and control over the standard creation for products they are importing.

THE VIRTUE OF COMPETITION

Lowered tariffs and easier market access bring about an increase in imports, which naturally escalates competition. The benefit of increased competition is that companies have to work harder (or smarter) to stay efficient, enhancing productivity of both economies and fostering a culture of innovation. Of course, in a more competitive environment, the least efficient companies are likely struggle to stay afloat.

ONE STANDARD, ONE TEST?

Despite all TTIP's professed benefits, the countries will need to overcome major hurdles to enjoy them. Apart from political uncertainties, both markets, embedded in their respective cultures, have developed their own licensing regulations, compulsory certifications and standards over decades. They have differing safety philosophies for product testing or certification that cannot simply be reduced to a common denominator.

What are the negotiators to do when it comes to discussing all the cases with differing norms for the same products? Which safety standards should they adopt within the agreement – the higher, or the lower ones?

THE SOLUTION BEGINS WITH TRUST

Ideally, a harmonized standard would include all worthy safety practices from both members to create a single comprehensive approach to ensure consumer safety. However, this does not mean that a single standard needs to be introduced. Nor is it absolutely essential to harmonize all standards for evaluating the safety of products.

Legislators, standard writing organizations and testing and certification companies across the Atlantic need to cooperate when it comes to testing and compliance methodology. A practical first step in the right direction is to have a Mutual Recognition Agreement. Mutual recognition only works well if both sides have confidence in the competence of the other certification body and acknowledge their know-how.

The second step is to establish Notified Bodies and allow them to perform conformity assessments and certification. It is also important to create uniform standards and apply comparable procedures when it comes to accrediting laboratories and appointing or licensing certification bodies to prevent the distortion of competition despite the free trade area.

Thus, the two markets will need mutual confidence – whether it concerns aligning existing regulations and allowing for mutual recognition of certification or cooperation on drawing up new national or international standards, if the latter should be necessary. Achievable and practical goals could be set as follows:

- Common rules, standards, and test procedures with the aim to establish uniformly high levels of quality and safety;
- Effective and efficient regulation of safety and testing standards on both sides of the Atlantic;
- Unburdening of the authorities by an independent conformity assessment system; and
- Strengthening the competences and expertise of standard setters.

Many independent testing and certification bodies are working now to make sure that future negotiations succeed in making the world a safer place. They will play a major role in establishing the success of what will surely be a very complicated and, at times, frustrating process of aligning more closely the different approaches to product safety standards and testing in the two markets. There is a strong support from the industry for a functioning and flourishing single market across the Atlantic, based on mutual trust and confidence.

(the author)

STEPHAN SCHMITT

As Chief International Officer of TÜV Rheinland AG, Stephan Schmitt has overseen business in the USA, Canada and Mexico since October 2011. An electrical engineering graduate of Trier University of Applied Sciences in Germany, he joined TÜV Rheinland in 1986 as a technical expert in Japan and has held various positions with the company ever since, including as CEO of TÜV Rheinland of North America.

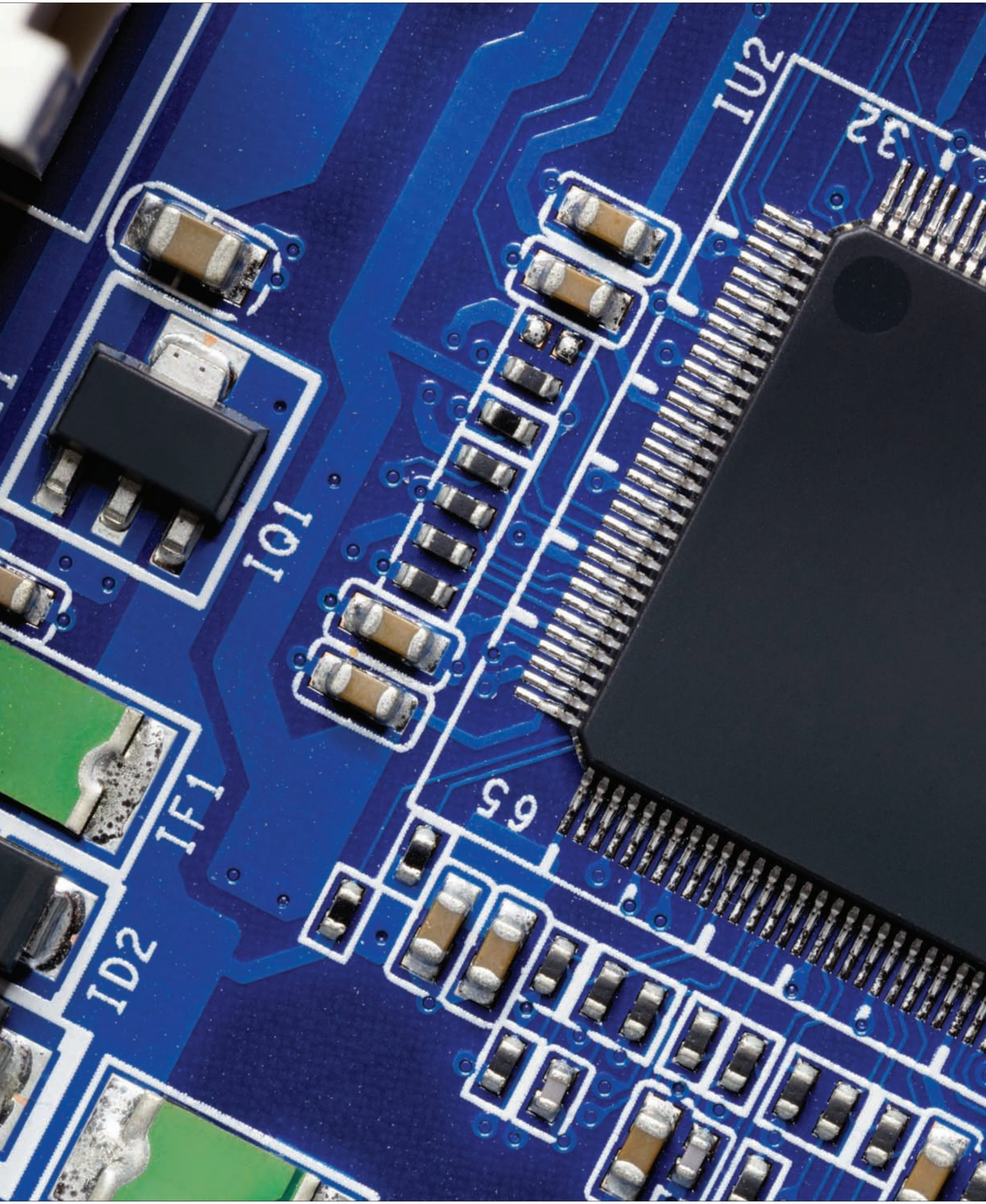

Differential Mode to Common Mode Conversion on Differential Signal Vias Due to Asymmetric GND Via Configurations

This article investigates the impact of ground vias placed in close proximity to high speed differential signal vias and the resulting differential mode to common mode conversion. The work shows the influence of the distance between ground (GND) vias and differential signal (Diff. SIG.); the effect of the asymmetrical configuration of the GND vias; the impact of the dielectric thickness and the number of transitions between the planes.

BY ALMA JAZE, BRUCE ARCHAMBEAULT, SAM CONNOR

Printed circuit boards (PCB) are continuously getting denser, more complex and have the need to meet operating requirements at higher frequencies. In order to deal with the very high speed digital communications, designers are often forced to use differential signaling to achieve acceptable signal integrity. This however has not reduced the need to control the EMI emissions. When high speed differential signals are routed on PCBs, the intention is to make the two parts of the differential pair as balanced as possible to insure low EMC emissions and high immunity to both external and internal noise. It is well known that any small amount of in-pair skew, rise/fall time mismatch, amplitude mismatch or any asymmetry can quickly create significant amounts of common mode noise on the differential signals lines, which then increases the EMI emissions [1]. Asymmetries in the wiring channels of the differential signals can cause differential-to-common mode conversion which can impact EMC emissions and common-to-differential mode conversion which can degrade system immunity to both internal and external noise sources.

These asymmetries extend to any asymmetry near the differential signal path, including differential vias near a ground-reference via. This work studies the mode conversion levels in the differential signal as a function of ground via distance, frequency, return via symmetry, number of reference planes traversed by the vias and the dielectric thickness. Differential mode to common mode (DM-to-CM) conversion can increase EMI emissions by coupling differential signals onto other vias, connector pins, etc. Common mode to differential mode (CM-to-DM) conversion is equal to

DM-to-CM and can cause external disturbances (such as ESD) to couple onto a differential signal as differential noise.

Full-wave analysis of entire boards can be very time consuming and often impossible due to the complexity, therefore analyzing simplified board designs can be helpful. Results from simple geometries can provide understanding of the underlying physics and can be used by most signal and power integrity design engineers as quick guidelines throughout the design process.

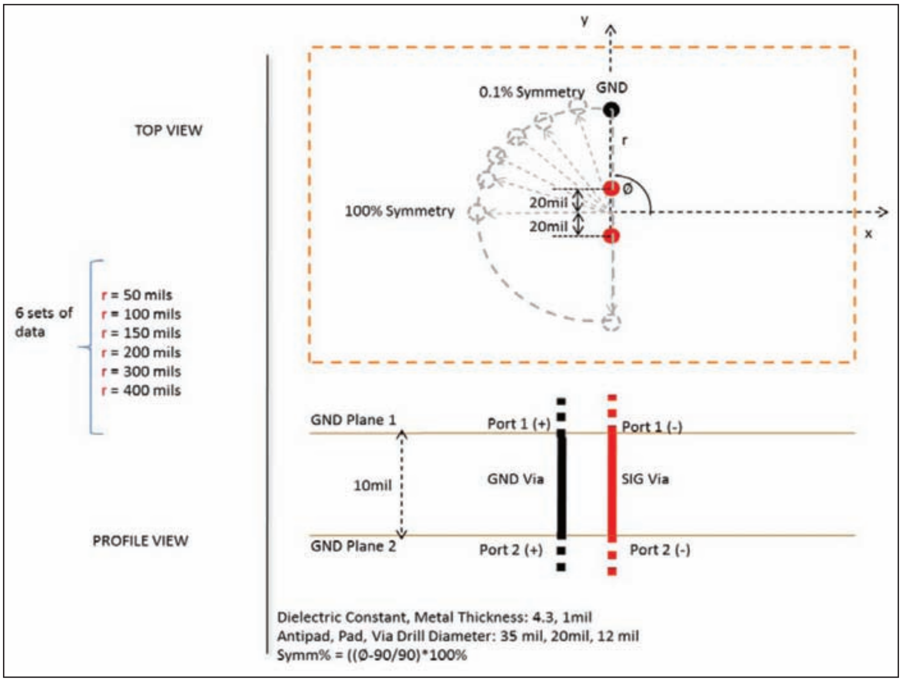

Figure 1: Layout of Models (Port 1 and Port 2 are mixed-mode ports)

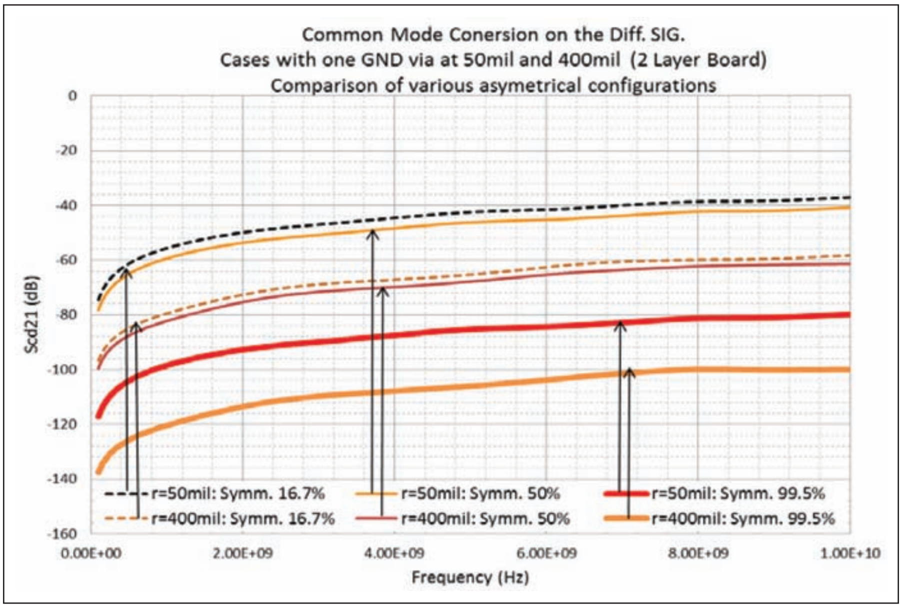

Figure 2: Common Mode Conversion (Scd21) for the case of best and worst symmetrical configurations

MODEL DEFINITION IN MULTILAYER VIA TRANSITIONAL TOOL

The cavity resonance approach to simulating effects between planes in PCBs has been demonstrated to be fast and effective [1], [2]. The Multilayer Via Transition Tool (MVTT) [2] was used as the primary simulation tool for this analysis. This tool is based on the cavity resonance approach and assembles each layer in multilayer PCBs to calculate overall results. It will model the power/ground plane cavities as rectangles (well-defined resonant modes) or infinite planes to avoid plane resonances that would limit the general applicability of the results to specific sized PCBs. In this study we have used infinite planes. This allows us to focus on the effects of ground vias without possible confusion from board size resonances. Figure 1 represents a cross sectional view of this model. The frequency range for which the S-parameters are calculated is 0.1GHz to 10GHz. A typical dielectric constant of 4.3 and metallic thickness of 1mil was used. The transfer function obtained between 0.1 GHz to 10 GHz from the MVTT simulations provides the amplitude of the DM-to-CM on the differential signal vias and traces. In all cases, a lower result (higher negative number) is desirable.

MODEL SIMULATION AND RESULT ANALYSIS

Case 1: Common Mode conversion for the case of one GND via placed in the vicinity of the Diff. SIG.

As mentioned above, we wish to quantify the mode conversion from the differential signal due to asymmetric ground via configuration. The common mode noise created will exist both in-between planes [3], [4], [5] and on the Diff. SIG. pair itself. The transfer function is obtained from the model

As expected, at higher frequencies there is more mode conversion for all cases than at the lower frequencies. The other thing to notice is that the best of the symmetry configurations also shows the least mode conversion by a significant amount.

shown in Figure 1 and is used as the basis for all the different sets of models that were used for data analysis.

The distance between the signal vias that make up the differential signal is 40 mils along the y-axis. The location of the ground via (GND1) is at a distance *r* from the origin, and its positioning relative to the y-axis changes from model to model. As the angular positioning between the GND via and the y-axis increases, so does the percentage of symmetry by which we quantify the symmetrical configuration of our model. When the GND via is aligned with the x-axis, we say that for this case we have 100% symmetry.

In Figure 2 the different curves represent different symmetrical configuration cases (i.e. 8% symmetry would be the worst case scenario and 99.7% symmetry would be close to the perfect symmetry scenario). As expected, at higher frequencies there is more mode conversion for all cases than at the lower frequencies. The other thing to notice is that the best of the symmetry configurations also shows the least mode conversion by a significant amount.

Common Mode Noise as a function of the distance of the GND vias from the differential signal

Figure 3 shows the effect of ground via distance and the best/worst case symmetry. We can observe that the distance of the ground via influences how much impact symmetry (or lack of symmetry) has on the transfer function.

Case 2: Common Mode conversion for the case of two GND vias placed in the vicinity of the Diff. SIG.

The plots in Figure 4 represent the simulation data for common mode conversion as a function of frequency and symmetry [5]. The location of the first ground via (GND1) is at a distance r from the origin, but always in line with the y-axis. While the second ground via (GND2) is also at the same distance r from the origin, its

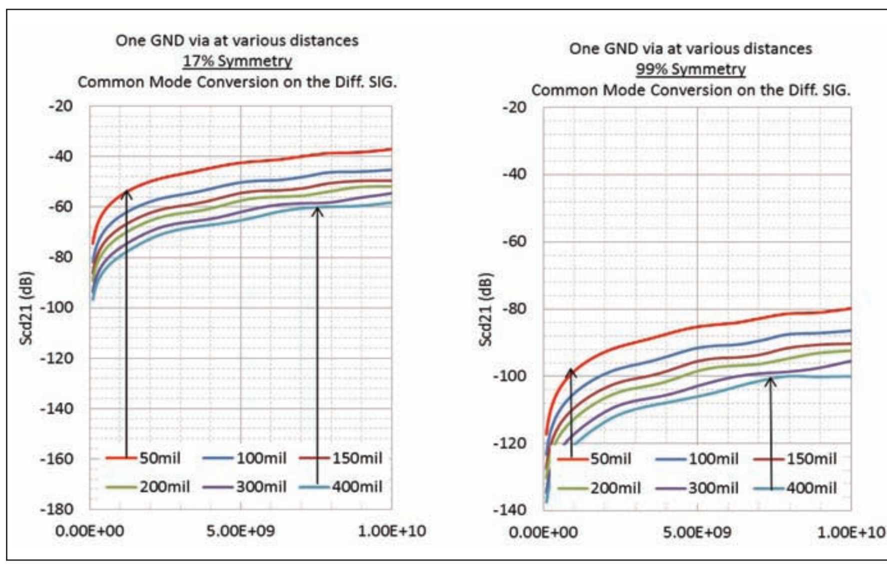

Figure 3: Mode Conversion for poor and good symmetry for various GND via distances.

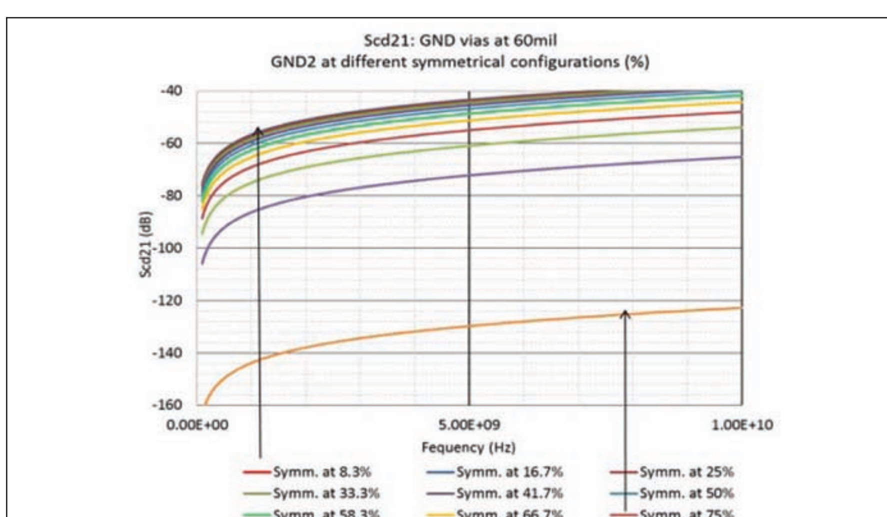

Figure 4: The effect of Asymmetry on Common Mode noise on the diff.signal

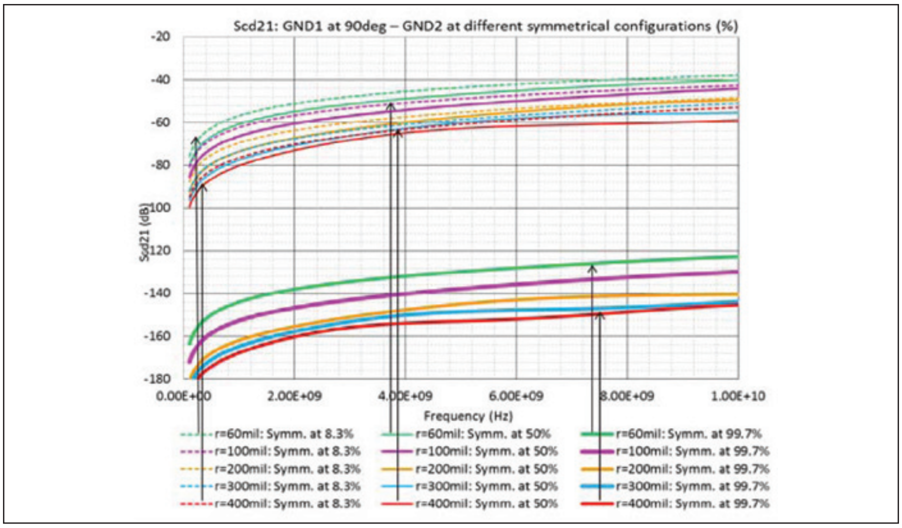

Figure 5: The effect of Asymmetry on Common Mode noise on the differential signal. Comparing different symmetrical configurations of GND vias when r varies.

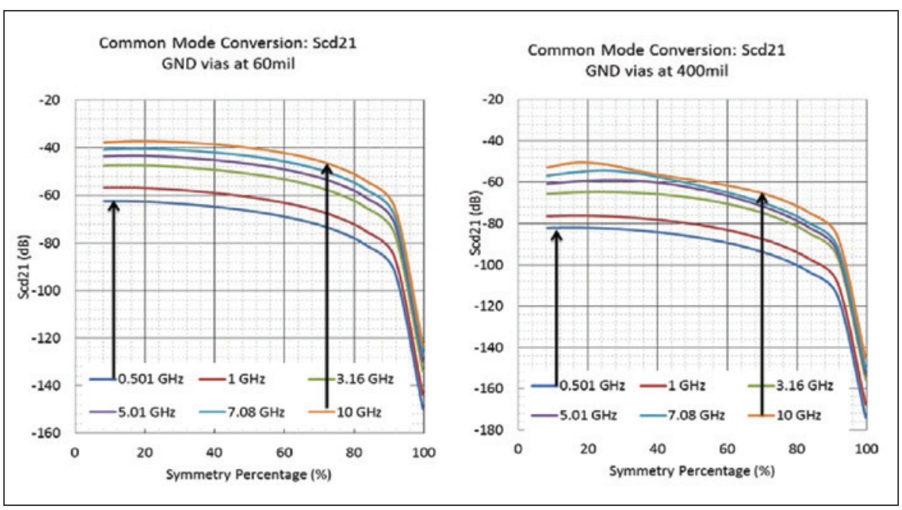

Figure 6: Differential to Common Mode conversion (Scd21) is greatly reduced if symmetry percentage is higher than 90%.

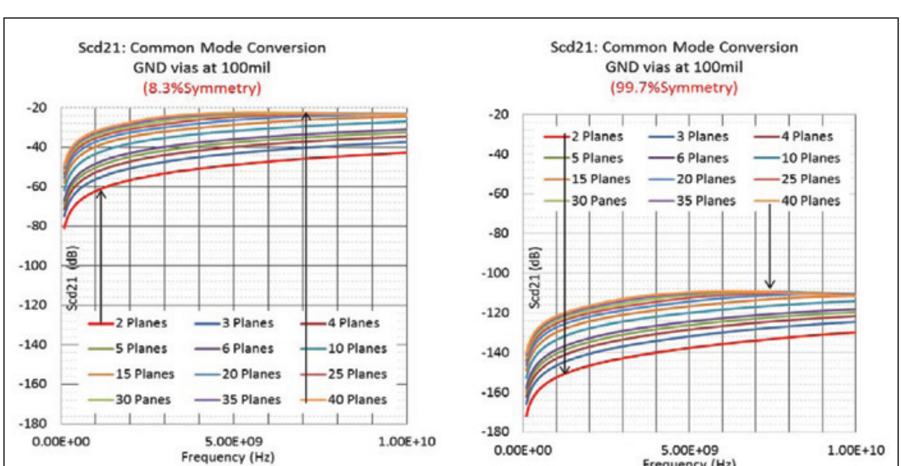

Figure 7: The effect of the number of planes on the common mode noise conversion

positioning relative to GND1 changes from model to model. As the distance between the two GND vias increases, so does the percentage of symmetry, by which we quantify the symmetrical configuration of our model. When both GND vias are aligned with the differential signal along the y-axis, we say that for this case we have 100% symmetry. Amongst the several values that were considered for the distance between GND vias and the Diff. SIG is the 60mils as shown in Figure 4. Common mode noise is highly reduced when the GND vias are close to perfect symmetrical configuration. The effect of the symmetry on the common mode noise as the distance between GND vias and the center of the Diff. SIG varies is shown in Figure 5. In Figure 6 where we are looking at the common mode conversion of just a few frequency points as a function of symmetry percentage. Amounts of mode conversion will vary based on the design requirements, however at 90% symmetry is where the curves show a substantial noise reduction.

Case 3: Mode conversion as a function of the number of GND planes for the case of two GND vias

In this section we have analyzed the mode conversion on the signal via-pair as the number of reference plane cavities traversed by the vias increases (as for thicker PCBs). In Figure 7 we have looked at the best and worst case symmetry cases of the GND vias relative to the Diff. SIG. As the number of planes increases, the Scd21 amplitude starts to converge. In Figure 8 we have shown how the change in Scd21 is affected by asymmetry (worst vs. best case) as the number of reference planes changes. We have picked several frequency points, and have shown the change in Scd21 as a function of the number of planes. At high frequencies, once convergence is reached there is very little variation in the change of Scd21 amplitude as the number of GND planes increases.

This work quantified the amount of mode conversion from differential mode to common mode, as the GND vias are asymmetrically placed near the differential signal vias. As expected, when the asymmetrical ground-reference vias are close to the Diff. SIG. vias the impact on the mode conversion is the greatest.

Case 4: The effect of symmetry on Scd21 for various dielectric thicknesses

In order to determine the effect of dielectric thickness, a number of different dielectric thicknesses were analyzed. The amplitude of the Scd21 varied with dielectric thickness, however the total difference between best and worst case symmetry configurations is approximately the same for all the various dielectric thicknesses (Figure 9). As the dielectric thickness increases, the impact of the GND via increases.

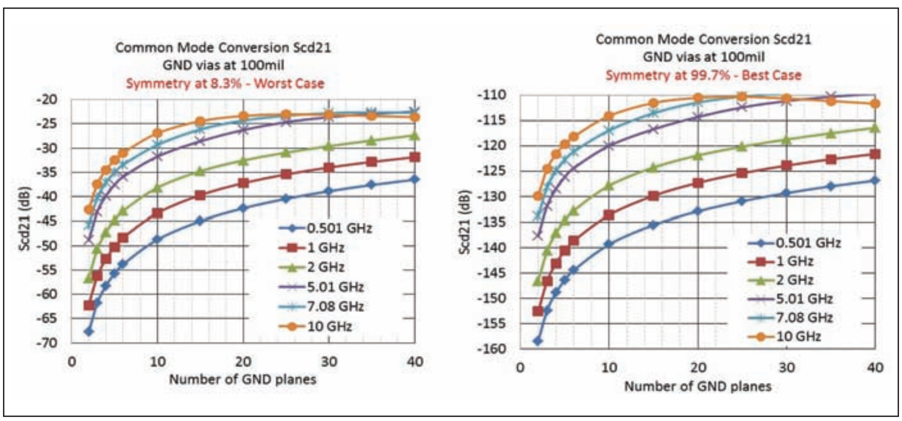

Figure 8: Common mode noise as a function of the number of planes through which the differential signal transitions

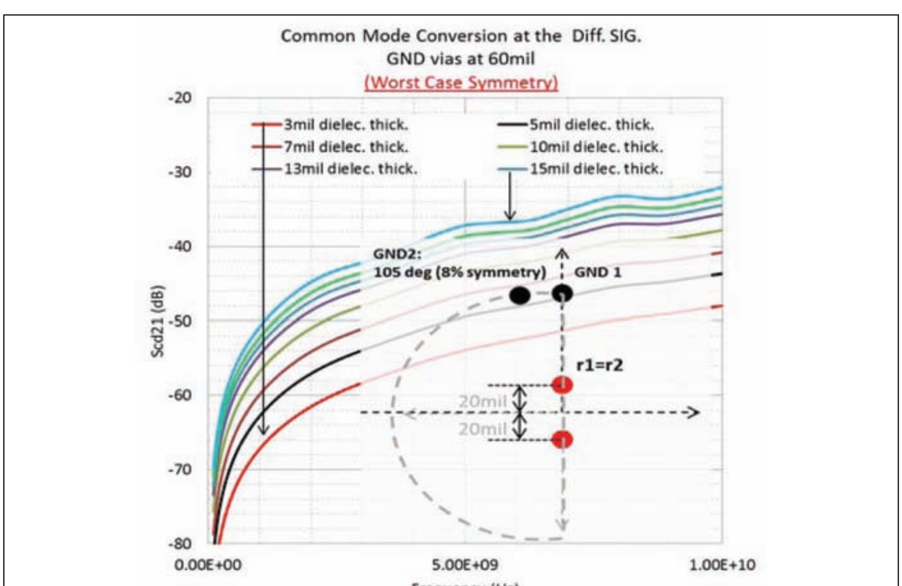

Figure 9: There is little to no change in the Scd21 amplitude amongst cases that correspond to different dielectric thicknesses.

CONCLUSION AND FUTURE WORK

This work quantified the amount of mode conversion from differential mode to common mode, as the GND vias are asymmetrically placed near the differential signal vias. As expected, when the asymmetrical ground-reference vias are close to the Diff. SIG. vias the impact on the mode conversion is the greatest. This would seem to imply that the ground-reference vias should be kept far away from the differential vias. This would be true only if the differential vias had no common mode noise on them from other sources. In reality, there will be some amount of common mode noise on the differential signals from PCB effects and/or silicon imbalances, so a ground-reference via in close proximity to the differential vias is required to allow the return current of this common mode noise to remain close to the matching noise current [4], [5]. Therefore, since a ground-reference via placed close to the differential vias is important and since the effect of ground-reference vias asymmetry is significant, the design rule becomes to maintain one or more ground-reference vias close to differential vias but to insure they are placed symmetrically with respect to the differential vias. Design guideline limits can be determined depending on the amplitude of the intentional differential signal and the transfer function.

The amount of mode conversion is not trivial! A 40 dB mode conversion factor means that a high speed intentional signal with a 1 volt signal could have a common mode noise amplitude of 10 mV. This alone could prove to be enough to cause a system to fail emissions testing if these differential lines are connected to unshielded cables through an I/O connector.

Another important point is the difference in the amount of mode conversion between good symmetry and poor symmetry. Figure 2 shows a 60 dB delta while Figure 4 shows as much as 80 dB difference. This is very significant and can easily make the pass/fail difference in systems with high-speed differential signals.

Future work will include other ground via configurations as well as optimization studies using tools such as genetic algorithms.

REFERENCES

1. Connor, S., B. Archambeault, and M. Mondal. "The Impact of Common Mode Currents on Signal Integrity and EMI in High-Speed Differential Data Links." *IEEE International Symposium on EMC*, (August 2008): 1-5.
2. de Paulis, F. , Y. Zhang, and J. Fan. "Signal/Power Integrity Analysis for Multilayer Printed Circuit Boards Using Cascaded S-parameters." *IEEE Transactions on Electromagnetic Compatibility*, vol. 52, no. 4, (November 2010).
3. Gu, X. , R. Rimolo-Donadio, Z. Yu, F. de Paulis, Y. H. Kwark, M. Cocchini, M.B. Ritter, B. Archambeault, A. Ruehli, J. Fan, and C. Schuster. "Fast Physics-Based Via and Trace Models for Signal and Power Integrity Coanalysis,. *DesignCon 2010*, Santa Clara, CA, (February 2010).
4. Jaze, A., B. Archambeault, and S. Connor. "EMI Noise Reduction Between Planes Due to a Signal Via with a Ground Via at Various Distances" *IEEE International Symposium on Electromagnetic Compatibility* (2011).
5. Jaze, A., B. Archambeault, and S. Connor. "Mode Conversion Due to Asymmetric GND Via Configuration." *IEEE International Symposium on Electromagnetic Compatibility* (2012).
6. Jaze, A., B. Archambeault, and S. Connor. "Effects of Nearby Ground Vias on High Speed Single-ended and Differential Signals." *DesignCon*, 2013.

(the authors)

ALMA JAZE
is an EMC Engineer at IBM in Poughkeepsie, NY. She graduated with a Master of Science in Electrical Engineering in 2006. While having already interned with IBM for three years (in Thermo Development and Power Development), upon graduation she became part of the EMC team. She is currently responsible for all EMC input throughout all phases of product design and development for the High-End Servers Division. In the most recent years, she has been involved in research work that focuses in PCB design effects and has a great interest in computational electromagnetics.

DR. BRUCE ARCHAMBEAULT
is an IBM Distinguished Engineer at IBM in Research Triangle Park, NC and an IEEE Fellow. He received his B.S.E.E degree from the University of New Hampshire in 1977 and his M.S.E.E degree from Northeastern University in 1981. He received his Ph. D. from the University of New Hampshire in 1997. His doctoral research was in the area of computational electromagnetics applied to real-world EMC problems. He is the author of the book "PCB Design for Real-World EMI Control" and the lead author of the book titled "EMI/EMC Computational Modeling Handbook".

SAM CONNOR
is a Senior Technical Staff Member at IBM and is responsible for the development of EMC and SI analysis tools/applications. Mr. Connor's current work activities and research interests also include electromagnetic modeling and simulation in support of power distribution and link path design for printed circuit boards. He has co-authored more than 20 papers in computational electromagnetics, mostly applied to decoupling and high-speed signaling issues in PCB designs. He is a Senior Member of the IEEE and is currently the Chair for the TC-9 subcommittee of the IEEE EMC Society.

The "Real" Cost of ESD Damage

BY TERRY WELSHER

Courtesy of The EOS/ESD Association, Inc.

Anyone who has worked in quality or reliability in a large corporation knows that developing and presenting credible failure cost information can be difficult. This is particularly true for ESD, where the events and their effects are invisible and not nearly as well understood as other more obvious classes of failure, such as mechanical or contamination.

The "real" cost of ESD can be a hot topic of discussion each year when program budgets are being developed for manufacturing and R&D programs. The challenge is that every year there are new high-level people in the financial and planning organizations who are not technical experts and are asking hard questions about the justification for the ESD investment. In years when revenue is down, the questions become more difficult and better evidence is often demanded. The author was directly involved in this process for 15 years, starting in 1986. At the time the following quote was a part of many ESD funding discussions "in the electronics industry, losses associated with ESD are estimated at between a half billion and five billion dollars annually." While the original reference for this assertion has been lost (to this author) it was used many times over the next few years in corporate presentations. While researching background information for this article, the exact same quote appeared (unattributed) in an article from 1992[1] and a book published in 2006[2]. Needless to say, a well-stated assertion of value can go a long way – at least in trade literature. However, this author can also report that the usefulness of such assertions, inside the corporation, eroded much faster. By 1990, a well-known director in Bell Labs said, "… that was then… I think this problem has been solved!" Many of us would scoff at such a declaration, knowing full well that ESD problems were continuing to occur. However, the director's challenge was an appropriate one. His experience came from the semiconductor process world where he had seen significant ESD sources eliminated, and device thresholds (albeit HBM only) steadily increase. Corporations wishing their investments to be justified by more timely and relevant data and observations ask, "What is the 'real' cost?"

Of course the immediate "real" cost information is very difficult to determine. In fact the use of the term *real* in the title reflects the collective skepticism ESD program managers and champions typically encounter. The $5 billion dollar loss number carries little weight in the final analysis. As a result, it is necessary to resist the temptation to assert an updated number for world-wide losses due to ESD. Instead, we revisit the general argument that ESD losses are potentially significant and that pressures that produced high failures rates (based on evidence published in the past), will increase with technology trends. The entire justification for the investment is really cost avoidance.

Making convincing arguments about potential losses have historically been very difficult as they must depend on studies done off-line or in the early days of implementation. In this article some of the important studies and articles that have appeared over the last 30 years regarding costs and benefits are reviewed. These include some classic split-lot experiments that showed the immediate impact of implementing an ESD program where none previously existed. In other more recent studies the investigators did not have the luxury of turning their program on and off, but nonetheless they were able to extract good information for the overall value proposition. There is no claim made here that this is a comprehensive collection of the most significant work. Rather, it represents studies that are known to this author and many colleagues and which are available as public information. There were many other proprietary internal studies which established the economic justification of programs that cannot be described here.

In 1989, the ESD Association published a collection of papers[3] from the first ten years of the EOS/ESD Symposium. This collection, *An ESD Management Focus*, was intended to provide ESD program advocates with a single source of significant work in supporting ESD programs and highlighting management issues. To this day it is still a useful source of information as 7 of the 19 articles in the collection directly address cost and benefits of the programs. Several of the studies are summarized here.

EARLY "SPLIT-LOT" EXPERIMENTS

At the time of the first EOS/ESD symposium in 1979 there were few mature ESD programs, but many companies were trying to establish them. Some of these companies were also developing their case for management through actual split lot experiments.

Western Electric Denver Works (1981)[4]

In this study the initial deployment of a basic ESD program was observed with careful collection of yield loss data for five key operations. Documented yield improvement up to 10.73% was observed, and with the assistance of the plant financial organization, the return-on-investment was estimated to be in the range of 900-2300%, depending on assumptions. This study was also significant in that it demonstrated that an effective program could be implemented in a very dry environment such as Denver, Colorado's without humidity control.

Western Electric North Andover Works (1983)[5]

This work included three separate definitive experiments on the effectiveness of ESD programs. Again, since ESD controls of any kind had not yet been implemented, simple split-lot experiments could be conducted. In these experiments as many as 1275 units were processed in a single experiment with and without controls. Clearly, it would be difficult to justify taking these risks today. Ratios of the number of failures in the unprotected and protected lots ranged from 1.9:1 to 5.5:1. The return on investment (for implementation of wrist straps and some ESD-protective transport materials) was as high as 950%. The quality assurance organization also studied the quality of outgoing product. The controls instituted in the factory resulted in a 3:1 reduction of defect rates.

Lockheed Missiles and Space Company (1983)[6]

In this study failure data before and after program implementation was collected, and explicit cost avoidance estimates were made. A detailed itemization of implementation and maintenance costs was weighed against extrapolated expected failure costs and an annual savings of almost $2 million/year was demonstrated.

No doubt there were many other studies done similar to these. The fact that no one is willing to risk doing these studies again is a testimony to the broadly accepted expectation that it would cost a lot of good product and precious production output. Some useful papers have also been published which describe in general terms how to gather cost information[7], estimate ROI[8], and provide basic understanding of the statistics of failure.[9]

CORRELATING PROGRAM EFFECTIVENESS AND YIELD

Studies that have followed the early split-lot work have had to detect the correlation between the strength of the ESD program and its effectiveness in improving yield. However, finding the data to support this correlation has proved difficult, as well. In one example[10] a factory was able to track ESD-related failures, as determined in Failure Mode Analysis, with deviations from specified procedures (Figure 1). It is rare that data can be de-constructed in this way, and there were some fortunate circumstances that allowed it in this case. In another very meticulous study[11] investigators were able to track yield at specific facilities and correlate it with the relative auditing scores. Based on this they were able to estimate the return-on-investment (3:1 in one study and 11:1 in another) of the specific procedures followed at the "exemplary" factories.

MISDIAGNOSIS OF ESD AS EOS

Understanding the cost of ESD requires accurate and timely Failure Mode and Root Cause Analysis. A relatively recent body of work suggests that some designations of failure modes need to be reconsidered. Most ESD testing and characterization of components is done on stand-alone parts. IC failure analysis data, which is usually based on knowledge of failure signatures seen in standard HBM and CDM tests, has caused many to conclude that ESD failures are relatively rare when compared to other electrical failures commonly classified as electrical overstress (EOS). Recent data and experience reported by several companies and laboratories now suggest that many failures previously classified as EOS may instead be the result of ESD failures due to Charged Board Events (CBE).[12] The reason for this is that boards may store considerably more charge than is stored by individual devices in the standard CDM tests. The resulting failure signature shows more physical damage (Figure 2) than a stand-alone device failure would and thus FA experts unfamiliar with this phenomenon often make the wrong diagnosis. In addition, similar observations have been made regarding the misdiagnosis of Cable Discharge Events (CDE) as EOS.[13] Some companies have estimated that about 50% of failures originally designated as EOS were actually CBE or CDE.

THE REAL "REAL" COST OF ESD – THE CRISIS

The studies described above, and many others like them, have served the advocacy of ESD program implementation well. While they are each very specific, it is easy to argue that the effects are general. They are also posed and conducted in terms that fit well with conventional financial metrics. However, the greatest costs due to ESD have come from a different source. Each of us who has been working in this area very long knows that the most obvious example of ESD cost is the *crisis*. When viewed this way an ESD program is more like insurance to shield the organization from disaster. Many of these crises have become the

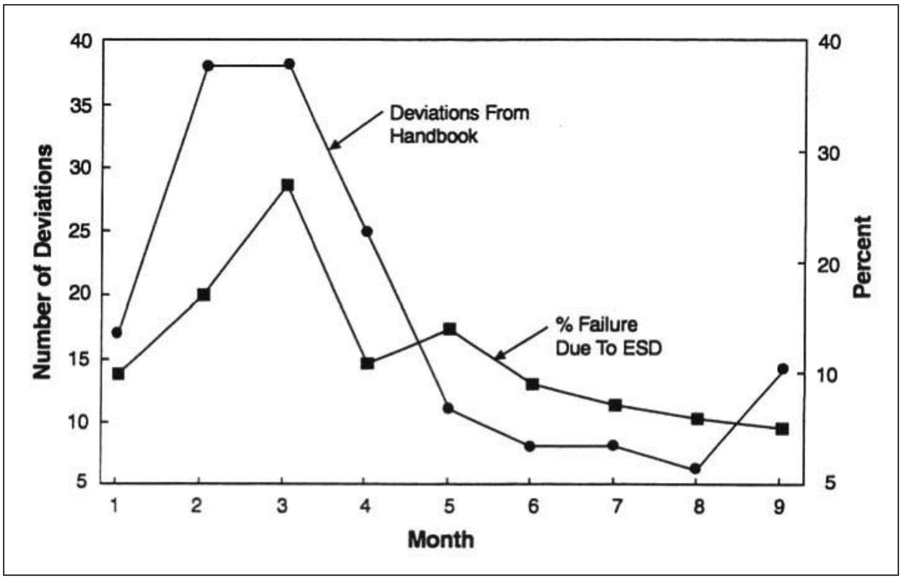

Figure 1: Correlation of ESD failure occurrence and deviations from ESD (Handbook) procedures

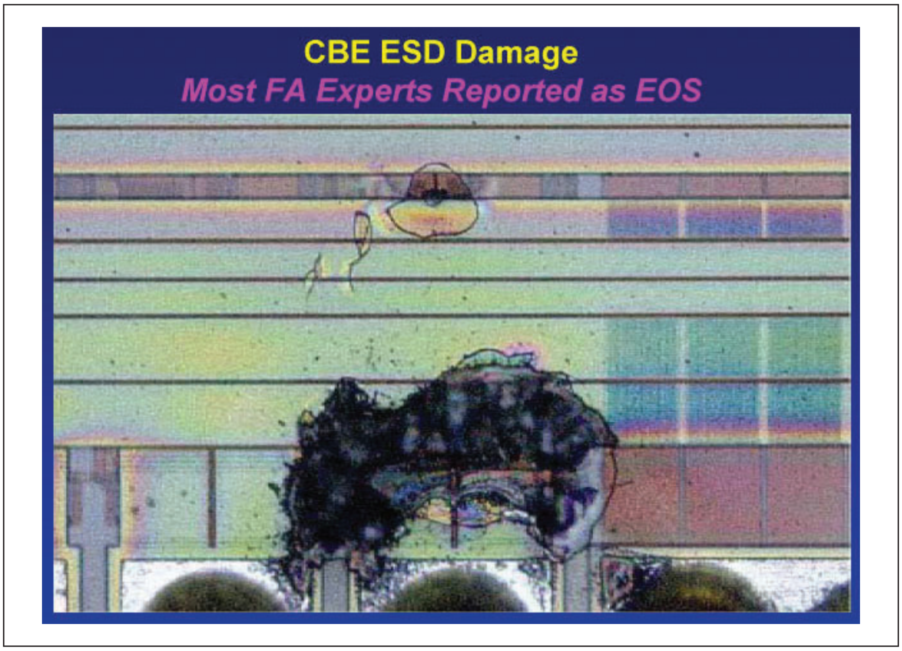

Figure 2: A charged-board ESD event failure signature resembles EOS

Crises affect a different set of metrics: productivity, time-to-market, time-to-profit, timely delivery and, of course, customer perception and confidence. This is why composite failure data is so misleading.

source of symposium papers and case histories. It could be argued that even if the ROI estimates from the studies above showed that the ROI was 1:1 or even a little less, most companies would still need good ESD programs. Crises affect a different set of metrics: productivity, time-to-market, time-to-profit, timely delivery and, of course, customer perception and confidence. This is why composite failure data is so misleading. A 1% of cost of sales failure level for ESD across the industry does not reflect the fact that perhaps 0.01% led to unacceptable damage to these other metrics. Some organizations go through cycles of crisis and cost reduction, particularly when there are management changes and a lack of long term data reporting.

EFFECT OF DEVICE THRESHOLDS – CONTROL/ PROTECTION BALANCE

Mitigation of ESD damage in electronics manufacturing depends on a dual strategy. In this discussion, the focus has been on the ESD control program. However, these programs would not be nearly as effective in maintaining high yield manufacturing if it were not for the parallel efforts of device designers to provide built-in ESD protection. This situation is illustrated in Figure 3. The front line in keeping yields high is at the point where devices become so sensitive that the "usual" procedures are not sufficiently effective. Of course experts are not in complete agreement as to where this point is and what additional controls are necessary. The hard disk industry certainly went through this point during the rapid evolution of MR head technology. Nanotechnology ICs may be approaching it. The point is that the risk of increased damage and higher costs will accelerate quickly as this regime is approached. The industry as a whole has arrived at a balance between these efforts, which are primarily driven by costs involved in the two parallel approaches, and which is weighed against the performance and function the customers are demanding, while of course maintaining a reasonable or decreasing product cost.

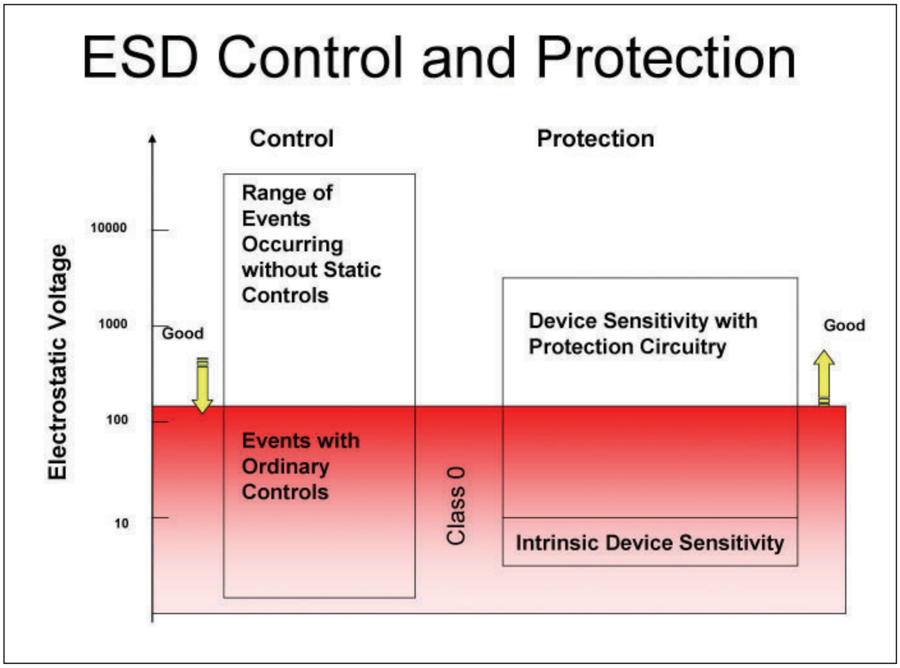

Figure 3: Cost effective programs balance factory control with built-in protection

For several years, this balance was tipped in favor of high device thresholds because the technology allowed it. Specifically, there had been a de facto standard of 2000 volts for the Human Body Model (HBM) ESD thresholds of integrated circuits. Recently an industry group, the Industry Council on ESD Targets, has issued two white papers addressing this issue for both HBM[14] and the Charged-Device Model (CDM).[15] These studies have demonstrated that the de facto targets, especially the HBM level, amount to substantially increased cost with little benefit. The increased cost of maintaining these targets in increasingly dense IC technologies results in very poor ROI. The studies on CDM, whose target was less widely used at about 500 volts, further suggest that improved implementation of CDM controls will be required. This is because the CDM targets for future technology nodes will at 250 volts and,

The International Technical Forum on Electrical Overstress and Electrostatic Discharge

September 7-12, 2014
Westin La Paloma Resort
Tucson, AZ, USA

Solve business challenges for controlling ESD by networking with other ESD professionals and industry experts.

Learn best practices and technology advances for ESD Control and protection design.

ESD ASSOCIATION

36th Annual EOS/ESD Symposium & Exhibits

- Two Emerging Technology Seminars are offered for the first time in 2014. The two seminars are scheduled for Monday afternoon and are being presented by leading experts in their field, who will give the attendees an excellent insight into GaN and 3D IC technologies.
- Ask the Expert Sessions for Device Testing and Factory & Materials. Industry experts will be on hand to discuss your questions in a free flow discussion format.
- Two "Year in Review" sessions on ESD On-chip Design and System-Level ESD.
- 37 Tutorials to keep you current organized in 4 dedicated tracks for ESD device design, IC ESD design, system ESD design and ESD control.
- Technical Sessions with over 50 engaging ESD presentations.
- Workshops for stimulating discussions on ESD Design, Factory Control, and Testing.

www.esda.org/symposiaEOS-ESD.html

EOS/ESD

In this article an attempt is made to bring the ESD value proposition up to date. The significant experiments done in the early development programs are relevant to today's processes.

for some high performance devices, 125 volts. Some 50 volt CDM parts are already being shipped.

CONCLUSION

In this article, an attempt is made to bring the ESD value proposition up to date. The significant experiments done in the early development programs are relevant to today's processes. On-going yield losses have been estimated and the operational ROI has been demonstrated many times to be significant. This alone suggests the investment in ESD control programs is a sound practice. The most significant effects, however, are the avoidance of crises, process excursions, downstream effects on higher value-added products, and maintaining positive customer perception. Technology trends suggest that the value of ESD control programs will increase and that more attention will be needed to maintain and improve them.

REFERENCES

1. *Sandia Science News.* (February 1992)
2. Trost, T. "Electrostatic Discharge (ESD) - Facts and Faults - A Review." *Packaging Technology and Science* 8 (1995): 231-247.
3. *An ESD Management Focus* EOS/ESD Association, (1989).
4. McFarland, W. Y. "The Economic Benefits of an Effective Electrostatic Discharge Awareness and Control Program – An Empirical Analysis." *EOS-3*, (1981): 28-33.
5. Dangelmayer, G. T. "ESD – How Often Does It happen?" *EOS-5*, (1983): 1-5.
6. Downing, M. H. "ESD Control Implementation and Cost Avoidance Analysis." *EOS-5*, (1983): 6-11.
7. Halperin, S. A. "Estimating ESD Losses in the Complex Organization." *EOS-8*, (1986): 12-18.
8. Allen, R. C. "ESD Control and ROI." *Evaluation Engineering*, (November 1999).
9. Moss, R.Y. "Cost Benefit Analysis – How Much Is Enough." *EOS/ESD Technology Europe*, (Spring 1990).
10. Dangelmayer, G. T. *ESD Program Management, 2nd Edition*, Springer, 1999.
11. Helling, K. "ESD Protection Measures Return on Investment Calculation and Case Study." *EOS-18*, (1996): 130-144.
12. Olney, A., B. Gifford, J. Guravage, A. Righter. "Real-World Printed Circuit Board Failures." *EOS/ESD Symposium Proceedings, EOS-25*, (2003): 34-43.
13. Dangelmayer, G. T., T. L. Welsher and A. Olney. "EOS versus ESD Misdiagnosis: Charged-Board Events Are a Growing Industry Concern." *Medical Electronics Manufacturing*, (Spring 2009).
14. Industry Council on ESD Target Levels. White Paper I: *A Case for Lowering Component Level HBM/MM ESD Specifications and Requirements.* (October 2010). www.esda.org/documents/whitepaper1_hbm_mm_2010.pdf
15. Industry Council on ESD Target Levels. *White Paper II: A Case for Lowering Component Level CDM ESD Specifications and Requirements.* (March 2009). www.esdindustrycouncil.org/ic/docs/JP_IndustryCouncil_WhitePaper2V1.0_Jan_2012.pdf

(the author)

DR. TERRY L. WELSHER

is currently Senior Vice President of Dangelmayer Associates. He began his career in Bell Labs in 1978 where he worked on electrolytic corrosion failure mechanisms in electrical interconnection materials. In 1986 he began directing Bell Laboratories' core expertise in electrostatic discharge (ESD). The newly formed group proceeded to produce a string of ground-breaking contributions to the field and played a key role in advancing industry standards. At his retirement from Lucent Bell Labs in 2001, he was Director of the Quality, Reliability and Test Center of Excellence. Dr. Welsher has served as Chairman of the ESDA Standards Committee and Technical Program and General Chair of the EOS/ESD Symposium. He is currently serving as President of the ESDA. He has also been active in the JEDEC Quality and Reliability Committee and Board of Directors and a member of the iNARTE Board of Directors. Most recently he has led the effort to harmonize and merge JEDEC and ESDA device testing standards. He holds a B.S. in Chemistry from Florida State University and Ph.D. in chemical physics from the University of Texas at Austin. Terry and his wife, Karyl, live in Suwanee, Georgia.

PRODUCT Showcase

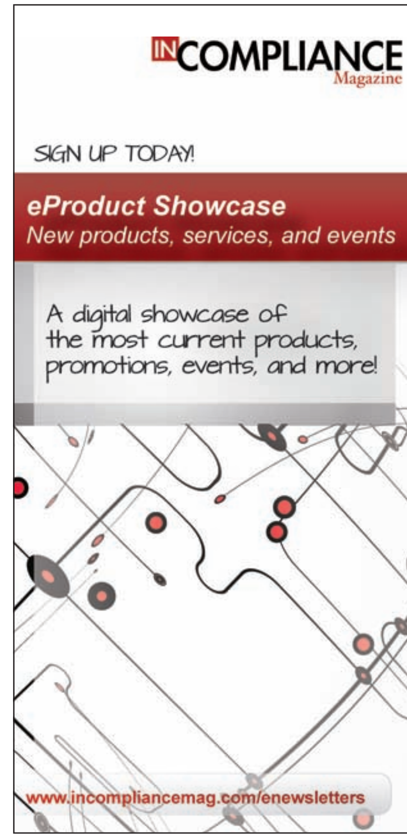

EVENTS in Compliance

June 2014

8
Understanding Ground Resistance Testing Training Seminar
AEMC Instruments
Syracuse, NY
www.incompliancemag.com/events/140708

9-10
Industrial Control Panels UL 508A and Short-Circuit Current Ratings
UL Knowledge Services
Fort Smith, AR
www.incompliancemag.com/events/140709

14-17
Understanding, Planning and Performing Climatic and Dynamic Tests to MIL-STD-810G
National Technical Systems
Santa Clarita, CA
www.incompliancemag.com/events/140714

15
Measurement, Control and Laboratory Use Equipment: IEC 61010-1 3rd Ed
UL Knowledge Services
Raleigh, NC
www.incompliancemag.com/events/140715_1

15-18
MIL-STD-461F Course
Washington Laboratories
Gaithersburg, MD
www.incompliancemag.com/events/140715_2

21
Achieving Precision Measurements
The Antenna Measurement Techniques Associationand IEEE Boston Chapters of the Electromagnetic Compatibility and Antennas and Propagation Societies
Waltham, MA
www.incompliancemag.com/events/140721

29-30
Industrial Control Panels UL 508A and Short-Circuit Current Ratings
UL Knowledge Services
Chicago, IL
www.incompliancemag.com/events/140729

BUSINESS News

ASSE's 2014 Triangle Award for Heroic Dedication Goes to Stefan Bright

The American Society of Safety Engineers (ASSE) is proud to announce Stefan Bright as the winner of the 2014 Triangle Award for Heroic Dedication for his role in establishing a field manual, training and standards that reduced fatalities among professional window washers by 30 percent over the last two decades. Bright, who received a record five Triangle Award nominations, is the safety director for Ohio-based International Window Cleaning Association (IWCA). Faced with increasing injuries and fatalities among window washers, Bright developed a field manual in 1992 outlining best practices. For more information, visit www.asse.org.

Connector from Amphenol Withstands Harsh Environments

Amphenol Industrial Products Group now offers a connector family with 1.5 mm socket contacts featuring Amphenol's RADSOK technology. Tru-Loc's rugged, compact, thermoplastic construction makes it ideal for use in harsh environments where high vibration and caustic fluids are present. Offered in a 2-way, 4-way or 6-way plug and receptacle in-line system, Tru-Loc is rated to 13 Amps continuous (with 16 gauge cable). It is designed to perform in demanding environments such as under valve covers on diesel engines to mate to fuel injectors. For more information, visit www.amphenol-industrial.com.

Applied Systems Engineering Introduces New Pulse/CW TWT Amplifier

Applied System Engineering has announced the introduction of model 277 TWT amplifier. It's a dual mode, grid pulsed and CW amplifier that provides 150 Watts at pulse widths from 0.05 μseconds to CW. The Model 277K frequency range is 18 to 26.5 GHz. The Model 277Ka frequency range is 26.5 to 40 GHz. The RF output pulse width tracks the input 5 volt video pulse. For more information, visit www.applsys.com.

Compact Vibration Table for Testing Small Components From Cincinnati Sub-Zero

Cincinnati Sub-Zero's (CSZ) new TCB-1.3 benchtop vibration table is ideal for reliability testing of compact products and electronics. The dual-purpose system is available in a 16" x 16" (40cm x 40cm) table size and may be used as a stand-alone vibration table for vibration testing or placed inside of an environmental chamber for combined vibration & temperature testing offering customers' flexibility and greater return on their investment. For more information, visit www.cszindustrial.com.

Delcross Technologies Releases Savant V4.0

Delcross Technologies announced the Version 4.0 release of its Savant™ software for modeling the installed performance of antennas on electrically large vehicles. With the introduction of Savant Version 4.0, Delcross provides the industry's only commercial asymptotic electromagnetic (EM) analysis software to extend the Shooting and Bouncing Rays (SBR) simulation approach with Physical Theory of Diffraction (PTD), Uniform Theory of Diffraction (UTD), and Creeping Waves. For more information, visit www.delcross.com

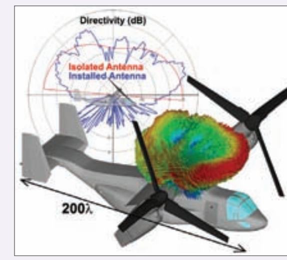

Intertek Awards Five $10,000 Scholarships and Internships to Engineering Stand-Outs

Intertek announced the first recipients of a scholarship and internship program targeted at undergraduate students pursuing studies in science, technology, engineering and math (STEM) in the U.S. and Canada. The Intertek Scholarship and Internship program provides up to $10,000 in scholarships, paired with an internship at an Intertek office, to five promising undergraduate students in the engineering field. Students who wish to apply for this scholarship and internship next year may visit www.intertek.com/scholarships for a full list of requirements and to learn more.

NexTek Releases Wide Band 2.2 GHz to 7.6 GHz Coaxial Lightning Protection for Wi-Fi, WiMAX, Satellite, LTE, & ISM Applications

NexTek, Inc. announced the release of a new line of SurgeGuard™ quarter wave stub lightning protectors. Designed specifically for LTE, Wi-Fi, and WiMAX applications, the QWS600 series exceeds 802.11, UNII, ISM and MIL-STD-202 standards for usage between 2.2 GHz and 7.6 GHz. OEMs have begun installing the QWS600 series in wireless applications that operate within this frequency range. For more information or a datasheet with complete product specifications, visit www.nexteklightning.com.

Pasternack Introduces New 1 Watt and 2 Watt Broadband Amplifiers Up to 18 GHz

Pasternack Enterprises, Inc. announced the release of ten new 1 Watt and 2 Watt broadband amplifiers, which are ideal for defense, EW/ECM, radar, test instrumentation, telecom, satcom, microwave radio and industrial applications from 2 GHz to 18 GHz. Pasternack's new medium power broadband amplifiers are offered in 1 Watt and 2 Watt models and range in frequency from 2 to 18 GHz depending on the RF amplifier configuration. For more information, visit www.pasternack.com.

York EMC Services Enhanced CNE III Kits Available from Reliant EMC

If you are a current owner of an CNE III from York EMC Services and would like to purchase additional CNE III's, this is your opportunity! The Enhanced CNE III Kit Includes: CNE III 9 kHz to 3.5 GHz comparison noise emitter, TLM01 (100 mm long top-loaded monopole, 200 MHz to 1 GHz optimum), TLM02 (270 mm long top-loaded monopole, 30 MHz to 300 MHz optimum), MCN01 monocone antenna (1 GHz to 3.5 GHz optimum with CNE III), LSA03 LISN adapter, manual, case and CAL01 (output power from 9 kHz to 5GHz measured using a spectrum analyzer). Contact Reliant EMC at (408) 600-1472 for more information.

New 52-Page Catalog for EMI/RFI Shielding Solutions From Tech-Etch

Available in both interactive PDF and printed versions, the 2014 catalog details all standard and custom EMI/RFI shielding product options. The easy-to-use PDF format lets the user jump from page-to-page with a mouse click to download interactive sales drawings of selected products. The 52-page catalog features to-scale technical drawings, compression values and metal thickness for over 100 BeCu and stainless steel finger stock shielding profiles. Visit www.tech-etch.com/shield to download the interactive PDF version.

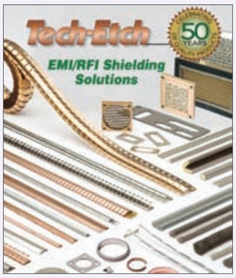

2014 NECR Code Changes Analyzed in Thomas & Betts' Free Reference Guide

Thomas & Betts (T&B) has published Analysis of NECR Code Changes 2014, a free reference guide to changes in the 2014 National Electrical CodeR (NECR) that pertain to T&B's products. This edition also covers code changes affecting ABB Low-Voltage Products (LP) and ABB Power Products. The 152-page guide is available as a print publication or it may be downloaded as an electronic PDF file. The book is organized by NECR article numbers with a table of contents, and includes illustrations of products and applications that pertain to code changes. Analysis of NECR Code Changes 2014 may be downloaded at www.public.tnb.com/pub/en/node/1890.

New Vishay Universal Edgewound Power Resistor

Vishay Intertechnology, Inc. introduced a new universal edgewound power resistor. Providing a convenient drop-in replacement for competing solutions, the universal-mounted EDGU combines a high-reliability design with continuous duty operation up to 85 A and a short-time overload of 10x rated power for five seconds. The Vishay Milwaukee EDGU features a resistance-alloy ribbon wire that is coiled on edge and supported on specially designed porcelain insulators, which provide proper turn-to-turn spacing and insulation from support bars. For more information, visit www.vishay.com.

(Authors)

DR. BRUCE ARCHAMBEAULT
is an IBM Distinguished Engineer at IBM in Research Triangle Park, NC and an IEEE Fellow. He received his B.S.E.E degree from the University of New Hampshire in 1977 and his M.S.E.E degree from Northeastern University in 1981. He received his Ph. D. from the University of New Hampshire in 1997.
For more about Bruce, visit page 47.

SAM CONNOR
is a Senior Technical Staff Member at IBM and is responsible for the development of EMC and SI analysis tools/applications. Mr. Connor's current work activities and research interests also include electromagnetic modeling and simulation in support of power distribution and link path design for printed circuit boards.
For more about Sam, visit page 47.

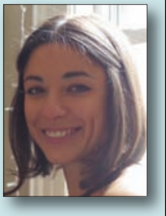

ALMA JAZE
is an EMC Engineer at IBM in Poughkeepsie, NY. She graduated with a Master of Science in Electrical Engineering in 2006. While having already interned with IBM for three years (in Thermo Development and Power Development), upon graduation she became part of the EMC team.
For more about Alma, visit page 47.

NIELS JONASSEN, MSC, DSC,
worked for 40 years at the Technical University of Denmark, where he conducted classes in electromagnetism, static and atmospheric electricity, airborne radioactivity, and indoor climate. Mr. Jonassen passed away in 2006.
For more about Mr. Jonassen, visit page 27.

AL MARTIN
Al holds a BEE degree from Cornell University, and a PhD from UCLA. Al joined Raychem in 1975, where he was initially involved with shielding effectiveness and surface transfer impedance measurements. Al went on to hold a number of positions, retiring in 2013.
For more about Al, visit page 35.

RICHARD NUTE
is a product safety consultant engaged in safety design, safety manufacturing, safety certification, safety standards, and forensic investigations. Mr. Nute holds a B.S. in Physical Science from California State Polytechnic University in San Luis Obispo, California.
For more about Richard, visit page 20.

STEPHAN SCHMITT
As Chief International Officer of TÜV Rheinland AG, Stephan Schmitt has overseen business in the USA, Canada and Mexico since October 2011. An electrical engineering graduate of Trier University of Applied Sciences in Germany, he joined TÜV Rheinland in 1986 as a technical expert in Japan.
For more about Stephan, visit page 39.

MIKE VIOLETTE
is President of Washington Labs and Director of American Certification Body. He can be reached at mikev@wll.com if you want to shoot the breeze.

DR. TERRY L. WELSHER
is currently Senior Vice President of Dangelmayer Associates. He began his career in Bell Labs in 1978 where he worked on electrolytic corrosion failure mechanisms in electrical interconnection materials. In 1986 he began directing Bell Laboratories' core expertise in electrostatic discharge (ESD).
For more about Terry, visit page 54.

We wish to thank our community of knowledgeable authors, indeed, experts in their field - who come together to bring you each issue of *In Compliance*. Their contributions of informative articles continue to move technology forward.

(Advertisers)

When Our Experience Goes in... EMI/RFI Noise Stays Out.

For reliable EMI/RFI shielding performance, turn to the most experienced manufacturer in the shielding industry: ETS-Lindgren. No other shielding company provides the product development, design/consultation, engineering expertise, and quality testing that result in the industry's most effective EMI/RFI protection from interference.

The ETS-Lindgren group of companies provides the industry's widest range of shielding systems and solutions, an unmatched understanding of proven shielding principles and techniques, and full service capabilities from design through certification.

For application assistance or to request our literature, visit our website at ets-lindgren.com.

We offer:

- Double Electrically Isolated (DEI) High-performance Screen or Solid Enclosures
- Cell Type Series 81/71 Shielded Rooms
- High-performance Welded Enclosures
- Series 101 Pan Shielding
- Highly-reliable Portable and Automated Test Boxes
- Automated and Manual RF Shielded Doors
- EMI/RFI Power/Signal Line Facility Filters

Enabling Your Success™

ETS·LINDGREN™

An **ESCO Technologies** Company

www.ets-lindgren.com

Phone +1.512.531.6400 • info@ets-lindgren.com

Offices in the US, Brazil, Germany, Finland, UK, France, India, Japan, Singapore, China, Taiwan


NSG 4070–75
Amplifier: 75 W 150 kHz – 230 MHz
TESEQ